UNITED NATIONS UNIVERSITY
UNU-GTP
Geothermal Training Programme

Orkustofnun, Grensasvegur 9,
IS-108 Reykjavik, Iceland

Reports 2017
Number 10

UPDATED CONCEPTUAL MODEL OF THE PATUHA GEOTHERMAL FIELD, INDONESIA

Elfina
PT Geo Dipa Energi (Persero)
Recapital Building 8th floor
Adityawarman Street Kav. 55
South Jakarta 12160
INDONESIA
elfina@geodipa.co.id

ABSTRACT

The 55 MW Patuha geothermal power plant is tapping steam from a vapour-dominated reservoir located in West Java Province of Indonesia. Systematic analysis of downhole data from the 31 deep and shallow wells drilled to date has produced initial pressure and temperature models for the extended resource area. The reservoir is split into four zones by their pressure potential. At top is a cold groundwater reservoir that extends down to about 1750 m a.s.l. Below is a clay cap, observed as a linear and conductive type thermal gradient down to elevations of 1050-1300 m a.s.l. The top of the productive high-temperature reservoir is located at this depth. The reservoir is mostly hosted within andesite, breccia and microdiorite intrusive rock. Matrix permeability may play a significant role in this lithological unit. A steam cap is encountered in its shallower part, underlain by a single-phase water reservoir of hydrostatic pressure. The steam cap has a thickness of 220-830 m. Its pressure ranges from as high as 50 bars at the Putih Crater, down to about 20 bars in the eastern wellfield. Such a lateral pressure gradient may relate to reservoir compartmentalization along faults that shift the reservoir host rock unit. The water-dominated reservoir has its top at 400-500 m a.s.l.; its details remain to be seen as most wells do not reach this depth. The updated conceptual reservoir model presented here is similar to previous ones with the exception of having the reservoir largely hosted by the same lithological unit. A single hot and magmatic upflow zone under the Putih Crater is proposed and compartmentalization is used to explain the lateral pressure gradient within the steam cap. Several maps of initial temperature and pressure distribution allow for estimating essential parameters for a volumetric generating capacity model. The extended reservoir area is between 6 and 20 km^2, its thickness is between 900 and 2000 m and the temperature ranges from 220 to 260°C. These model parameters yield a generating capacity in excess of the currently installed 55 MW. Due to the vapour-dominated nature of the resource, a more detailed 3D model should be applied, in particular, to study the behaviour of the liquid dominated section during long term production. Modelling studies of other vapour-dominated fields on Java suggest that steam caps like that of Patuha are supported by their underlying liquid water zone. Long term resource management should consider this.

1. INTRODUCTION

The Patuha geothermal field is located in Bandung and Cianjur Districts, West Java Province, Indonesia, around 50 km to the southwest of Bandung (Figure 1). Java island is located adjacent to the convergent plate boundary, and the tectonics control the major structural trends of the island (Figure 2). Patuha concession area is around 350 km^2, excluding Cibuni concession area, which is inside the Patuha concession area (Figure 3). There are many thermal surface manifestations such as fumaroles, which appear in Ciwidey, Cibuni, and Putih Crater, mud pools in the eastern part of the field, hot springs appear

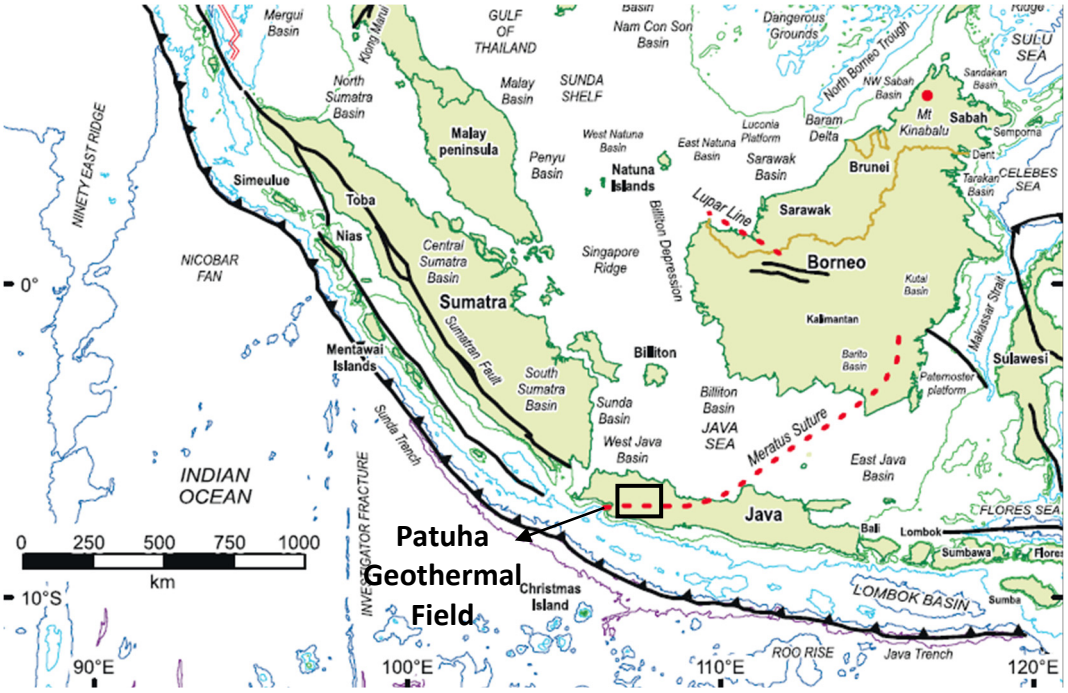

FIGURE 1: Location of Patuha geothermal field and tectonic features in the western part of Indonesia (modified from Hall, 2012)

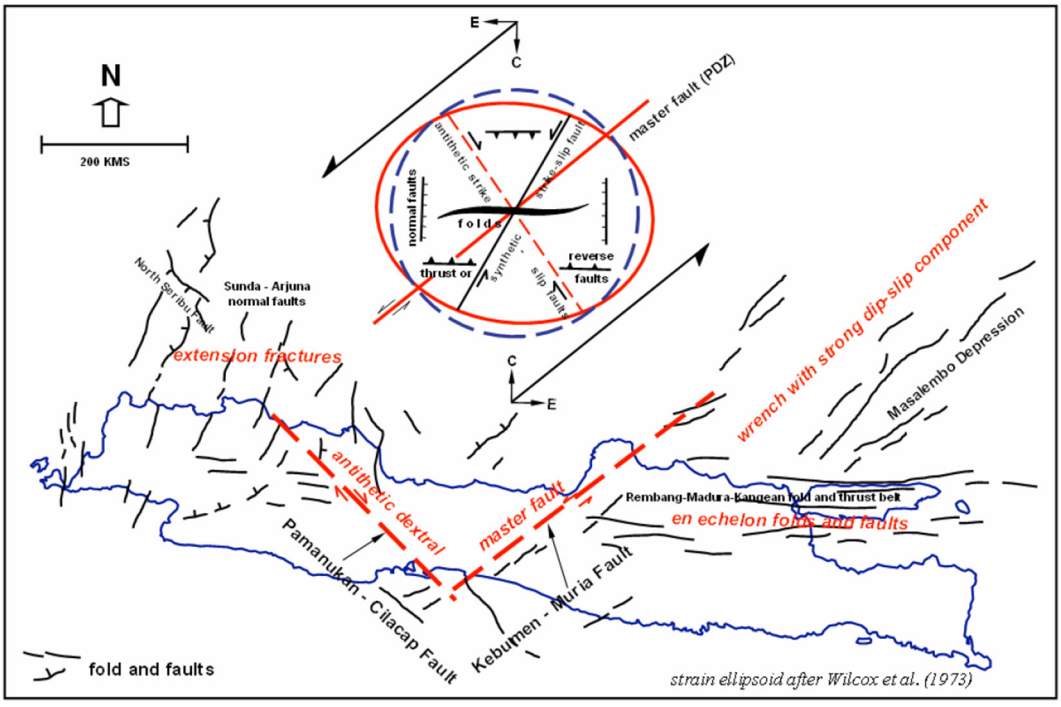

FIGURE 2: Structural trends on Java Island (Satyana, 2007)

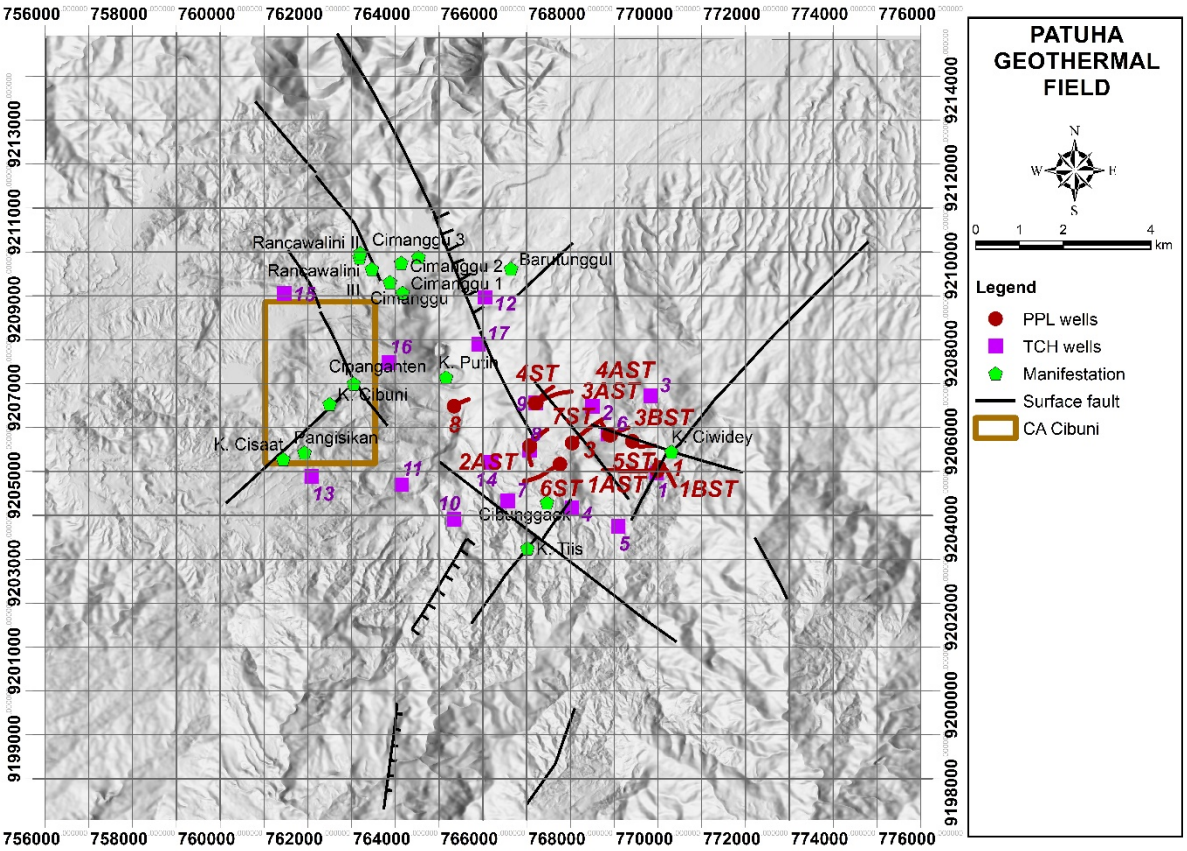

FIGURE 3: Structural map of Patuha geothermal field, showing also location of wells and geothermal manifestations

in the northern, eastern, western parts of the field, and warm springs appear in northern, western, southern parts of the field (Figure 3).

Drilling was started by Patuha Power Ltd. with a slim hole campaign in 1996 (17 wells). The field development continued through drilling large and standard diameter wells until 1998 (14 wells). Due to the Indonesian economic crisis, the exploration drilling was stopped in 1998. The Indonesian government assigned PT Geo Dipa Energi to develop geothermal power plants in Dieng and Patuha in 2002. In 2011, PT Geo Dipa Energi constructed a steam gathering system and a power plant for the 55 MW Patuha Unit 1. The Commercial Operation Date (COD) for Patuha was in September 2014.

Monitoring of the production wells for the last three years shows some changes, particularly a decline of the wells. The challenge is to maintain the steam supply to have a stable capacity at 55 MW. Updating conceptual and numerical models can help to arrange the reservoir management strategy, including a plan to drill make-up wells.

This report will discuss an updated conceptual model for Patuha. It is structured as follows. After describing the regional and local geological setting, a brief outline is given on the Patuha geochemistry and geophysics. The bulk of the work performed is described in a chapter on the downhole data analysis, resulting in initial pressure and temperature profiles for most wells. These data are then plotted in planes and cross-sections, together with reservoir subsurface stratigraphy. A cross-correlation with other information available is made, resulting in an updated conceptual reservoir model. Some essential reservoir parameters such as the reservoir area extent, thickness, and temperature range are finally used to develop a volumetric generating capacity model for Patuha. The report ends with conclusions. A supplementary report details the estimation of initial temperature and pressure estimates (Elfina, 2017).

2. REGIONAL GEOLOGICAL SETTINGS

Patuha geothermal field is located in Java Island, which is a part of the Sunda Land and adjacent to the convergent boundary plate between the Eurasian Plate and the Indo-Australia Plate (Figure 1). The rate of subduction of the Indo Australia Plate beneath the Eurasian Plate is 6-7 cm/year, with the highest rate in West Java. This subduction, which developed in the early Tertiary, has controlled the volcanic activity in West Java and also the structural trend. In Java, there are four different structure-trends (Figure 2), i.e. N-S (Sunda trend), NE-SW (Meratus trend), E-W (Java trend), and NW-SE (Sumatera trend). The age of the structures from the oldest to the youngest is Meratus trend (Late Cretaceous), Sumatera trend (Late Cretaceous to Paleocene), Sunda trend (Late Oligocene), and Java trend (Early Miocene). The Sumatera, Meratus, and Sunda trends consist of normal and strike-slip faults, while the Java trend consists of thrust-reverse faults and folds (Pulunggono et al., cited in Fauzi et al., 2015).

In West Java, surface and deep seated structures have a different trend. Based on the regional geology map, the N-S and NNE-SSW trends represent the surface structure. Based on the regional Bouger anomaly, the NW-SE and WNW-ESE trend represent the deep seated structure. Regional structure has the role to provide permeability as the extensional setting for fluid accumulation in the reservoir and controls the distribution of the heat source or volcanism (Fauzi et al., 2015). The trend for the extensional setting is varied at NNW-N-NNE (Fauzi et al., 2015), such as in Wayang Windu, which has the most permeable fault, striking 40° and 310° (Bogie et al., 2008).

3. LOCAL GEOLOGICAL SETTINGS OF THE PATUHA GEOTHERMAL FIELD

There are ten production wells, two injection wells, two idle wells, and 17 slim core holes in the Patuha field. The production, injection, and idle wells are located in eight pads. Most of the production and injection wells are located in the eastern part of the concession and the idle wells are located in the centre of the concession (Figure 3). The names of the production, injection, and idle wells always start with PPL (Patuha Power Limited) and for core holes they start with TCH. To make their names still visible, only the number of the wells are shown on the map.

The Patuha geothermal field is surrounded by a volcanic centre or vents which are distributed along a west to northwest trending structure (Layman and Soemarinda, 2003). Based on field mapping reports, general structure trends that develop in this field are NE-SW and NW-SE, which are the Meratus and Sumatera trends. Regional tectonics influence the structure in this field, the compression from north to south produces a NW-SE dextral strike-slip fault, sinistral NE-SW strike-slip fault, and a N-S normal fault (Figure 3). There are six NW-SE dextral strike-slip faults, i.e. the Rancabali fault, Patenggang fault, Ciwidey Crater fault, Urug fault, Tiis fault, and Dewata fault (Figure 3). There are five NE-SW sinistral strike-slip faults, i.e. the Alamendah fault, Cibuni Crater fault, Ciwidey Crater fault, Tiis fault, and Dewata fault. There are three normal faults, i.e. Putih Crater fault, Curug Ciayun fault, and Narunggul fault. Based on field data in Ciwidey Crater, sinistral strike-slip faults formed before the dextral strike-slip faults (LAPI ITB, 2014).

Strike-slip faulting is a product from compression tectonics, therefore they tend to have lower permeability compared to normal faults. If a strike-slip fault is reactivated as a normal fault, the permeability of the fault tends to increase (Bogie et al., 2008). The Ciwidey Crater fault is not only a sinistral strike-slip fault but also a normal fault that developed in the last stage. Presumably, this fault is a reactivation of a strike-slip fault that increased the permeability, as shown in surface manifestation such as fumaroles, mud pools, and hot springs. The Ciwidey Crater appeared in the intersection of dextral Ciwidey Crater fault and the sinistral Ciwidey Crater fault. This can also affect the permeability in the sinistral Ciwidey Crater fault. Other manifestations such as the Tiss Crater, Cibuni Crater, and Cisaat Crater also appear controlled by a north-easterly trending structure such as a strike-slip fault.

There is no evidence of vertical movement of the fault in the field. Nevertheless, appearance of the manifestations in those craters can also indicate that the fault has a good permeability.

Figure 4 outlines the main geological units, with most of the field surface covered by Quaternary volcanic products from Mount Kendeng and Mount Patuha (Koesmono et al., 1996). The youngest is a product from Mount Patuha (Q_v), and consists of lava and lahar pyroxene andesite. The product from Mount Patuha is overlain by a product from Mount Kendeng (Q_l), which consists of intercalated lava with a laharic deposit of andesite breccia and tuff breccia. In the south and south-eastern parts of the field, the surface is covered with undivided pyroclastic deposits (Q_{Tv}), which consist of andesite breccia, tuff breccia, and lapilli tuff. An outcrop of Tertiary sedimentary rock was found in the south (Koleberes formation) as well as Tertiary volcanic rock (Beser formation). These Tertiary rocks are probably the basement of the geothermal system (Figure 4).

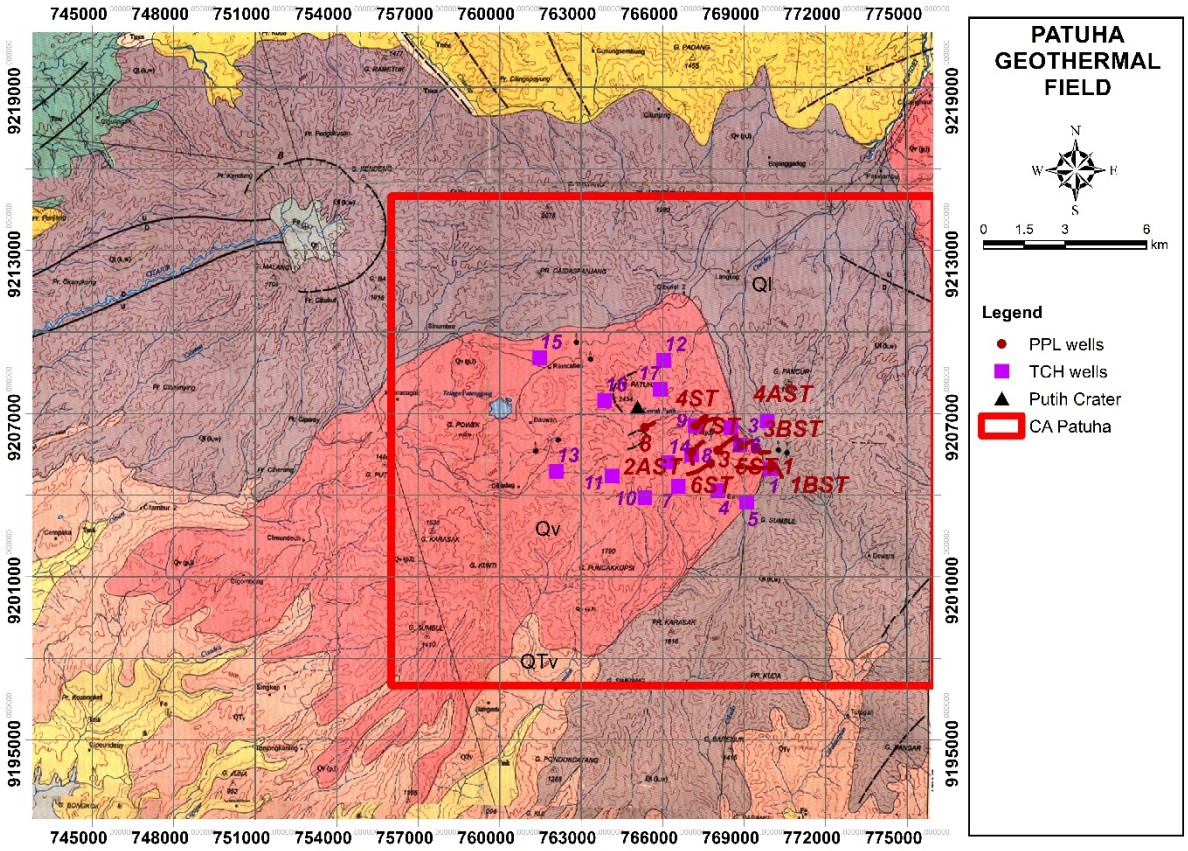

FIGURE 4: Geological map of the Sindangbarang and Bandarwaru quadrangles, Java, including Patuha geothermal field (modified from Koesmono et al., 1996)

Systematic analysis of drill cuttings from the formation evaluation logs and lithology summary reports of 14 wells, produce a simplified lithology that consists of andesite lava, andesite-dacitic lava, lithic tuff, andesitic breccia, tuff breccia / breccia, andesite complex and microdiorite as an intrusion. The Q_v lithology unit can be identified as andesite lava intercalated with lithic tuff (pyroclastic), andesite, and andesite-dacitic lava. Q_l lithology unit in the wells consists of thick andesite, lithic tuff (pyroclastic), andesite breccia, and tuff breccia. Q_{Tv} lithology unit in the wells consists of andesite complex (lava andesite associated with microdiorite), andesite breccia, and breccia/tuff breccia. There is no data that mentions Tertiary rock in either formation evaluation logs or lithology summary reports. However, the regional geology map (Koesmono et al., 1996) shows the Tertiary rock outcrop in the southern and northern part of the field (Figure 4). The geology is discussed more in Section 8 below.

4. GEOCHEMISTRY OF THERMAL MANIFESTATIONS

Manifestations in Patuha consist of fumaroles, mud pools, hot springs, warm springs, and cold springs with or without cold gas discharge (Figure 3). The active Putih Crater is related to boiling, acidic hot springs, and fumaroles. The colour of the lake is greenish white and has a connection with the acid gas vent in the bottom of the lake, as sulphur deposits can be found around the lake. Based on monitoring from 1995 to 1997, the pH trends inversely correlate with total sulphur. The pH of the lake is between < 0.5 and 1.3 (Sriwana et al., 2000). The distinctive characteristic fluid in this crater compared to other craters nearby, is the content of magmatic gases and a high content of chloride. Other fumaroles, hot springs and mud pools can be found in Ciwidey (eastern part of the field) and Cibuni Crater (western part of the field). The Cimanggu hot spring and the Barutunggul and Rancawalini, warm springs appear in the northern part of the field. The Cibunggaok warm spring and a cold spring in Tiis Crater with cold gas discharge appear in the southern part of the field. The hot springs in Ciwidey and Cibuni Crater are steam heated water and Cimanggu hot spring is bicarbonate water.

Gas geothermometers are widely used to support reservoir conceptual models and predict deep reservoir temperatures. The results of gas geothermometers (log (H_2/H_2O) vs log (H_2/N_2)) indicate almost the same results as from logging data in deep wells, which is a temperature between 220 and 240°C (PWC et al., 2013). Other geothermometers with CO_2-H_2S-CH_4-H_2 from the steam composition in several wells have been studied and showed a temperature range between 226 and 245°C. Gas geothermometers H_2-Ar and CO_2-Ar show the reservoir temperature exceeding 250°C. Moreover, gas geothermometer CO_2-H2 shows high temperature, over 270°C beneath wells 02AST, 03BST, and 04ST. Wells 04ST and 02AST are situated close to the Putih Crater, which is assumed be the centre of the system. This range is higher than the measured temperature in the well. Oxygen and hydrogen isotope analysis indicate that the isotope value is similar to the local surface water. It shows that the origin of the geothermal fluid is meteoric water and also affected by steam or steam condensate (JBIC, 2007).

5. GEOPHYSICAL STUDIES

A gravity survey was conducted in 1996 with 528 stations (Geosystem, 1995 and 1996). The results of this survey are presented in Bouguer anomaly and residual anomaly maps. In these maps, gravity lineaments of WNW-ESE orientation are evident (PWC et al., 2013). The maps also show a central volcano which is the main deep structure which controls the geothermal activity in Patuha (Layman and Soemarinda, 2003). The Bouguer map shows a gravity-high anomaly in the southwestern part and a gravity-low anomaly in the northeastern part. A gravity high points to the area being lava dominant and a gravity low is probably related to Tertiary rocks and sediments in the northeastern part of the field (PWC et al., 2013).

A MT survey was conducted in 1983 by CGG/GEOCO with 139 MT stations. Geosystem and PTI Tri Bawana Utama did an addition survey with 35 MT stations in 1995 and finally in 1997 Geosystem and PTI Tri Bawana Utama did another survey with 85 MT stations. A TDEM survey was conducted with 255 stations to be able to apply a static shift correction to the MT data. The latest 2D MT inversion model was done by Elnusa in 2013. The results show several cross-sections with N-S and NW-SE lineations, and two lineations with a W-E direction (the data is not shown in this report). The model shows low resistivity values of under 10 Ωm that indicate cap rock or intense argillic alteration (clay cap). The thickness of the cap rock tends to increase towards west-northwest and decreases around Ciwidey Crater. The result from the 2D MT inversion in the W-E direction shows low resistivity compared to the surrounding area, which has high resistivity values beneath Putih Crater. This high-resistivity plume is assumed to be a upflow zone with magmatic gases toward Putih Crater (Figure 5). This section shows the distribution of the reservoir from west to east and also shows the upflow from the heat source. This section is used in cross correlating the geological cross-section and in putting forward a conceptual model later in the report.

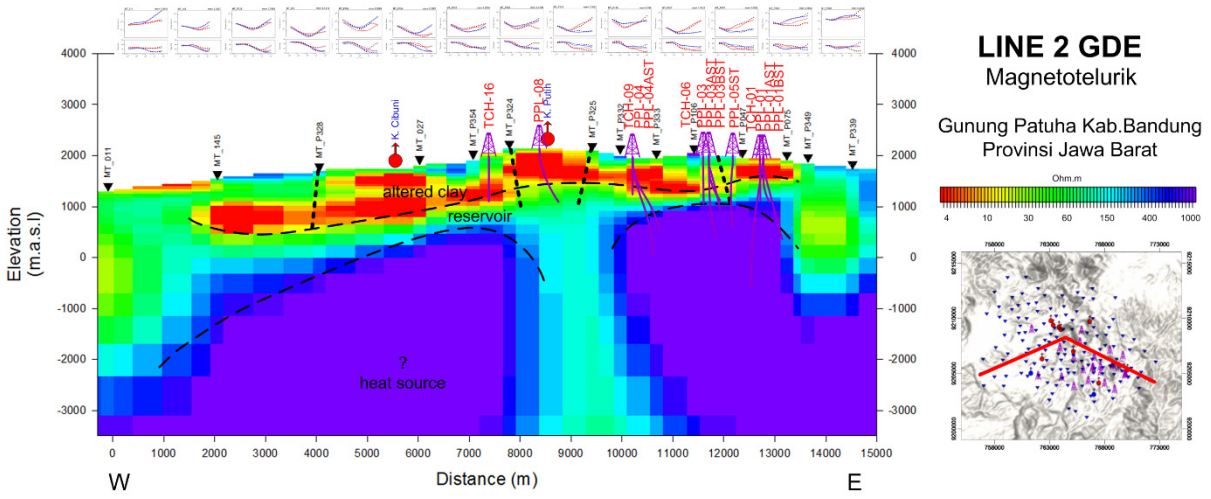

FIGURE 5: W-E MT 2D cross-section through Patuha (Elnusa, 2013)

6. ANALYSIS OF DOWNHOLE DATA

There are in total 14 deep wells in Patuha. These include production, injection, and idle wells, which are situated in the central and eastern part of the field. Additionally, there are 17 TCH slim wells in the area (Figure 3). Pressure temperature (PT) logging has been done to monitor the heating-up of wells and during injection from 1996 to 1998, after that the wells are in shut-in or bleeding conditions. A PT survey was conducted in 2003 and 2010 in bleeding condition and the last logging was in 2015 after one year of production.

To analyse the downhole data, a primitive database has been developed, including:

- 121 downhole temperature logs;
- 117 downhole pressure logs;
- Well summary reports, well schematics, formation evaluation logs, and daily drilling reports for 14 wells;
- Three reports regarding geological surveys and a feasibility study report.

With the well data in place, the next step was to collect and compile all the PT logs and plot into a single graph for each well. This was then combined with the schematics of the well, feed zone data (Total Loss Circulation (TLC) zone, Partial Loss Circulation (PLC) zone, Drilling Break (DB) zone, and spinner log), simplified lithology, and mineral alteration (clay and epidote). In these graphics, TLC is marked with black triangles, PLC is marked with white triangles, and DB is marked with grey squares (Figures 6 and 7). Note that the data analysis performed here is extensive, it generated a lot of graphics and contains data which some have confidentiality restrictions. Another, supplementary report therefore presents these data in more detail (Elfina 2017).

The second step of the data processing is to estimate the initial temperatures and pressures, which can then be used as a baseline for the natural state model. In some cases, the downhole temperature and pressure data do not show the actual formation condition due to a cooling process while drilling and the time needed for heating-up. Furthermore, alteration data assist in understanding the evolution of the reservoir, particularly in identifying the top of reservoir (TOR). The key minerals being considered in this report are clay and epidote, especially the top of clay (TOC), top of epidote (TOE), and top of continuous epidote (TCE), explained as follows:

- TOC can be used to indicate the top of cap rock.
- TOE is determined at the first appearance of epidote, the appearance of this mineral is not continued in the next interval depth, and sometimes there is another appearance in the several hundred metres after the first appearance of epidote.
- TCE is determined with the appearance of epidote becoming relatively stable at some interval depth. In general, epidote can be used as a key mineral to infer a propylitic alteration zone associated with temperatures above 240°C (Reyes, 2000).

6.1 Initial temperature and pressure in well 02

Well 02 is a production well that is located in Pad 2 at an elevation of 2011 m a.s.l., near the centre of the field, around 2.6 km distance from Putih Crater. The isothermal profile in the shallow part is interpreted here as a shallow groundwater zone (Figure 6). About 620 m thick cap rock zone is inferred from the difference between TOC and TOR, and secondary mineralogy and a linear thermal gradient (conductive zone) in the same depth interval. The TOR is set at an elevation of 1229 m a.s.l., where the convective zone starts as a vapour phase. The thickness of the vapour-dominated zone is around 720 m. Underneath the vapour-dominated convective steam cap, pressure goes back to hydrostatic. Thus, the horizontal layering of the reservoir is that of shallow ground water zone and hydrostatic pressure, followed by a cap rock layer of linear thermal gradient and sub hydrostatic pressure and a steam cap that is hosted under the cap rock, finally underlain by single-phase water reservoir.

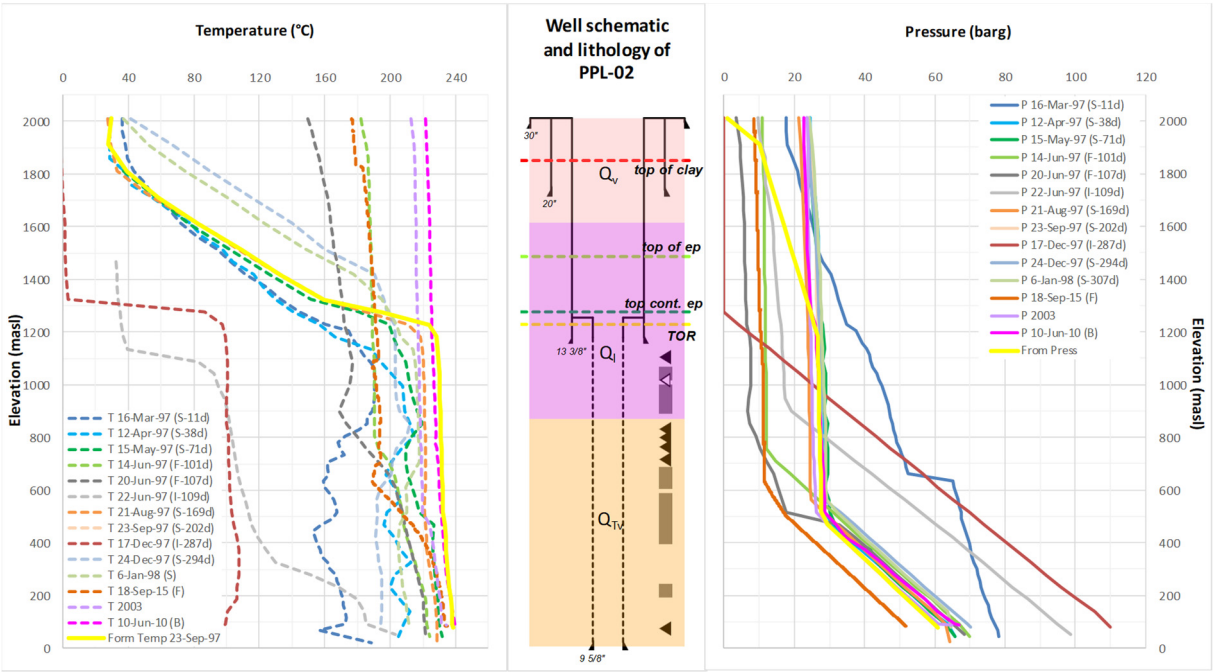

FIGURE 6: Temperature, pressure, lithology and design of well 02

The maximum measured temperature is 238°C at the bottom of the well, at an elevation of 78 m a.s.l. Logging data from September 1997 within the reservoir is higher than the water saturation curve until 517 m a.s.l. formation temperature in the reservoir is predicted as the highest temperature measurement in 1997. Main feed zones are located at elevations of 1095, 1043, 754, 700 and 626 m a.s.l., being indicated by TLC and confirmed with spinner data. The steam cap pressure is predicted around 27 barg from elevation 1182 to 517 m a.s.l. where the pressure goes to hydrostatic and then increases until 60 barg at the bottom of the well. Slightly increasing temperature and TLC at the bottom of the well suggest another feed zone there. The assumption of sub-hydrostatic pressure in the cap rock is based on connecting the hydrostatic pressure linearly in the shallow well and the steam cap pressure at TOR. The reservoir and feed zones are hosted within the Q_l and Q_{Tv} lithology units. The TOE is at an elevation of

1486 m a.s.l. and the TCE at an elevation of 1274 m a.s.l., both are above the TOR vapour dominated zone. This suggests a gradual process of the reservoir moving from initial hydrostatic pressure to the present vapour static pressure behaviour.

6.2 Initial temperature and pressure in well 04ST

Well 04ST is a production well located in Pad 4 at an elevation of 1968 m a.s.l., near the centre of the field, around 2.2 km distance from Putih Crater. The isothermal profile in the uppermost part indicates a shallow groundwater zone (Figure 7). The thickness of the cap rock is about 776 m from TOC to TOR, also showing up as a linear thermal gradient (conductive zone). No PT logs exist that clearly show the TOR, so it is assumed that the elevation of the TOR is similar to other wells. The TOR is probably at an elevation of 1100 m a.s.l., where the convective zone starts and vapour is found.

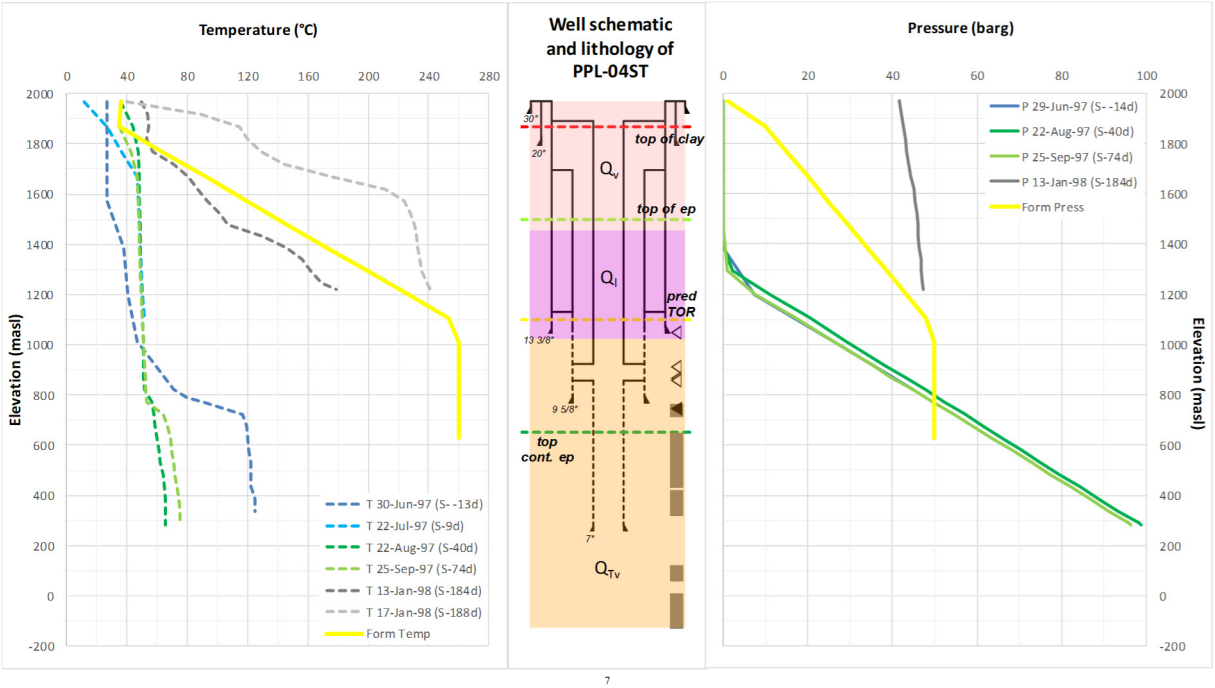

FIGURE 7: Temperature, pressure, lithology and design of well of well 04ST

The maximum measured temperature in the well is 241°C at an elevation of 1219 m a.s.l., but the logging tool could not reach the bottom of the well. The latest PT logging was done in 1998 or 184 days after drilling. According to the data, it is believed that the well may need more time to heat up, so the data from 1998 are not representative of the formation condition. The main feed zone, which is indicated by the TLC (Total Loss of Circulation), is at an elevation of 749 m a.s.l. The maximum pressure, which was recorded on 13 January 1998, is 48 barg at an elevation of 1218 m a.s.l. This pressure is the highest pressure recorded at this elevation in the field. From data collected nearby in 1998, it is assumed that the well has a connection with the reservoir and has a vapour zone at the same elevation as nearby wells. Therefore, the estimated reservoir temperature reaches 260°C and the pressure reaches 50 barg at saturated conditions. The assumption of the pressure in the cap rock is based on the hydrostatic pressure in the shallow part (assumed shallow groundwater) and linear interpolation to the top of reservoir. The reservoir and the feed zone are probably hosted within the Q_l and Q_{Tv} lithology units. The TOE is at an elevation of 1489 m a.s.l. and the TCE at an elevation of 649 m a.s.l., only the TOE is above the TOR for the vapour-dominated zone. This explains the fluid phase change in the reservoir from the initial hydrostatic to the current vapour static. No further analysis about 04AST is made here as the well did not reach the liquid-dominated reservoir.

6.3 Analysis of the initial temperature and pressure profiles with depth

The current work initially focused on one deep well at a time. With all wells being investigated, a second round of initial temperature and pressure estimates was made. The aim was to fine-tune the thickness of the cap rock in each well, cross correlating the estimates with neighbouring wells and finally pushing the limit by estimating initial temperature and pressure in deep wells with limited data by relying on the mineralogy as a marker for TOC and TOR.

In addition to the deep well analysis, downhole temperatures in the slim thermal gradient wells were gathered. As these wells are not in pressure communication with the deep reservoir, only initial temperature estimates are presented here. Figure 8 plots all initial temperature and pressure profiles in the deep Patuha wells, and in Figure 9 the initial temperature estimates are shown for all the slim thermal gradient wells. The depth reference is always relative to sea level for easier cross correlation. Table 1 shows the values of initial pressures and temperatures for all the deep wells and Table 2 shows the initial

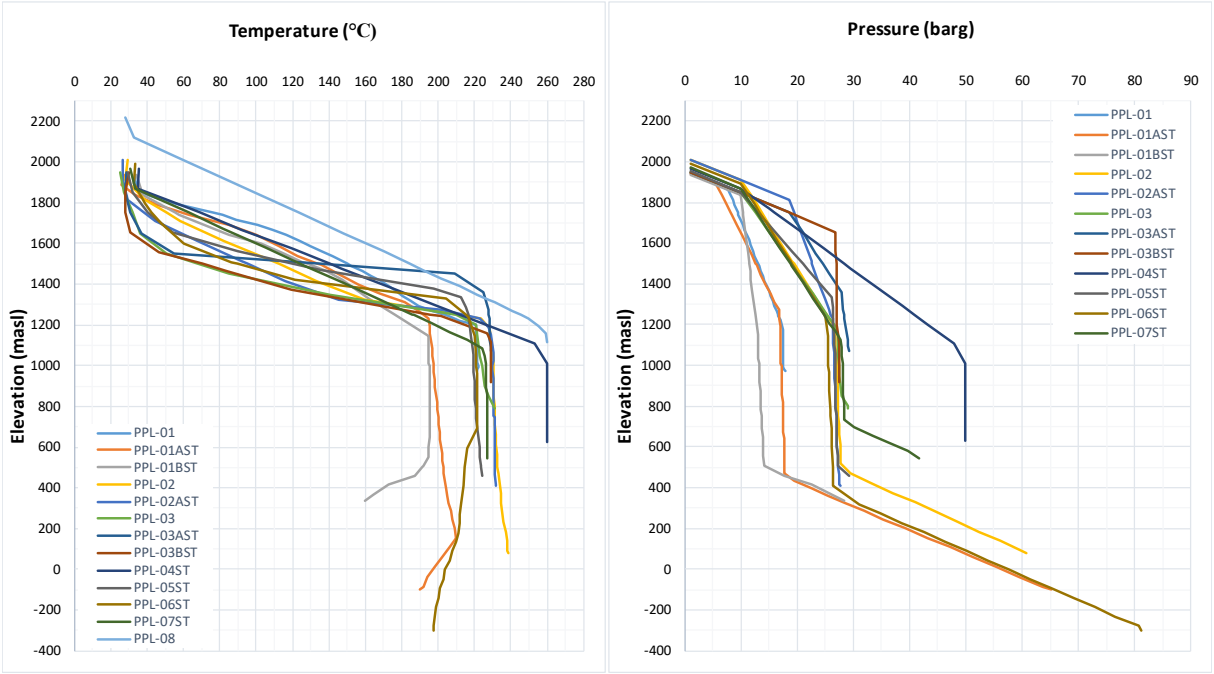

FIGURE 8: Comparison of initial temperature and pressure in deep wells

TABLE 1: Initial temperature and pressure for all the deep wells

Elevation (m a.s.l.)	PPL-01		PPL-01 AST		PPL-01 BST		PPL-02		PPL-02 AST		PPL-03		PPL-03 AST		PPL-03 BST		PPL-04 ST		PPL-05 ST		PPL-06 ST		PPL-07 ST		PPL-08	
	T	P	T	P	T	P	T	P	T	P	T	P	T	P	T	P	T	P	T	P	T	P	T	P	T	P
1750	76	9	59	8	55	10	51	14	38	19	32	13	31	19	28	19	69	16	40	13	43	13	63	13	123	n/a
1500	150	13	133	13	128	11	112	19	95	23	68	19	135	24	70	27	140	28	120	21	90	19	124	19	185	n/a
1250	204	17	192	17	176	13	211	25	214	26	210	25	228	28	195	27	212	41	217	26	215	25	186	25	246	n/a
1000	222	18	197	17	195	13	230	27	230	27	224	27			229	27	260	50	219	27	221	26	226	28		
750			200	17	195	14	231	27	231	27							260	50	221	27	222	26	227	28		
500			203	18	191	15	233	28	232	27									223	27	215	26				

TABLE 2: Initial temperature (°C) estimates for all the slim hole wells

Elevation (m a.s.l.)	TCH-02	TCH-03	TCH-04	TCH-05	TCH-07	TCH-09	TCH-10	TCH-11	TCH-12	TCH-13	TCH-14	TCH-15	TCH-16	TCH-17
	T	T	T	T	T	T	T	T	T	T	T	T	T	T
1750	21	28	28	23	45	47	39	30	51	n/a	37	n/a	37	82
1500	77	48	69	62	90	106	61	57	75	46	70	36	92	157
1250	127	86	117	99	133	159	83	91	119	96	116	65	151	217
1000	173	130	163	134	175	220	107	124	162	138	160	96	208	270
750	226	170	210	170	218	281	130	158	203	182	204	125	260	270
500	226	200	210	207	218	281	153	191	220	225	240	156	270	275

temperature estimates for all the slim holes. Note that the deep well names begin with a number while the slim thermal gradient wells have an "S-" prefix.

From the discussion above and the profiles in Figure 8, the characteristics of the 13 wells can be divided into three groups:

1. Group 1 includes all wells in Pad 1, consisting of 01, 01AST, and 01BST. These wells have a steam cap pressure around 16-17 barg and a reservoir temperature of 222°C.
2. Group 2 includes all wells in Pad 2, Pad 3, Pad 5, Pad 6, and Pad 7. Their steam cap pressure is around 25-29 barg and the reservoir temperature ranges from 221 to 231°C.
3. Group 3 includes wells 04ST and 08, the steam cap pressure here may go as high as 50 barg and the predicted reservoir temperature is around 260°C.

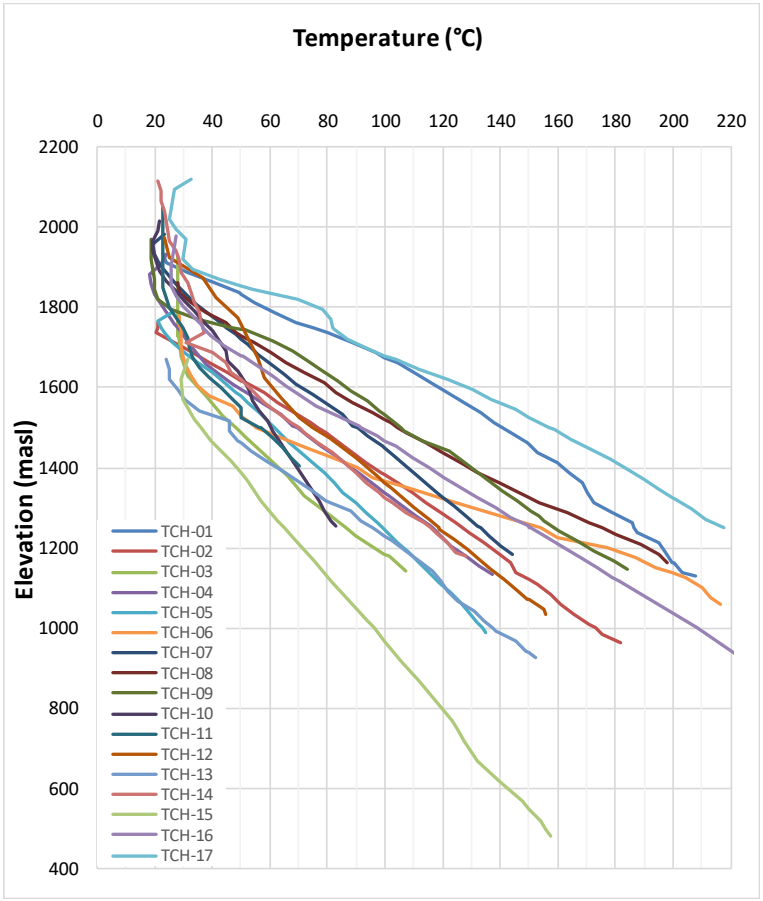

FIGURE 9: Comparison of temperature in slim hole thermal gradient wells

The slim hole data is plotted together in Figure 9 to see the gradient temperature in the shallow part. Furthermore, these wells show the area extent of the reservoir and its outer boundaries. By selecting 1000 m a.s.l. as a reference depth, being close to the base of the clay cap, and extrapolating the linear gradient in wells that are completed just slightly of this elevation, it allows dividing them into three groups:

1. Temperature < 150°C: S-03, S-05, S-10, S-11, S-13, and S-15;
2. Temperature 150-200°C: S-02, S-04, S-07, S-12, and S-14;
3. Temperature >200°C: S-09, S-16, and S-17.

As seen in Figure 8, the Patuha deep geothermal reservoir can be divided into two zones, the upper vapour-dominated zone, and the deeper liquid-dominated zone. Most production wells are tapping the vapour-dominated zone only, but several wells also enter the liquid zone, such as 02, 02AST, 01AST, 01BST, 06ST, 07, and 05ST. Based on data from nine wells, the thickness of the vapour-dominated zone ranges from 217 to 827 m and this reservoir section is the main steam contributor for the current power plant.

The deep liquid zone could be presented as a "dead leg" in most wells if producing dry steam only. PT surveys while flowing show the indication of a fluctuation in the flashing level. In addition to that, chemical analysis from the downhole samples also show that the steam phase has a chemical connection with the deep reservoir, which is also hotter than the steam cap (Layman and Soemarinda, 2003). Spinner data from 2015 for well 02 confirms that the liquid zone also contributes while flowing at low well head pressures (WHP). Therefore, it can be inferred that the underlying liquid zone supports the steam to the vapour-dominated zone. Based on data from seven wells, the liquid zone is found at an elevation of 400-500 m a.s.l. Most of the wells produce dry steam with an enthalpy over 2700 kJ/kg, except 02, which

has an enthalpy range of 2065-2760 kJ/kg (Table 3). The high enthalpy in 02 was recorded with the WHP 11.5 barg with a water fraction of 0.01 and the lowest enthalpy was recorded with WHP 8.6-8.9 barg with a water fraction of 0.35.

The analysis of initial temperatures and pressures with depth in Patuha is supported with various additional information, such as well design and drill cutting analysis, the estimation of reservoir flashing levels. As a good housekeeping measure, most of these assumptions have been collected in a standard form and are tabulated in Table 3 below.

TABLE 3: Summary of information from 14 deep wells

Well	Status	Location of liner		Top of clay (m asl)	Top of res. (m asl)	Boiling level (m asl)	Feed zone (m a.s.l.)	Enthalpy (kJ/kg)	Shut-in pressure (barg)	Remarks
		TOL (m a.s.l.)	BOL (m a.s.l.)							
PPL-01	Prod.	1194	959	1895	1199	n/a	1012, 996	2802	16.6	Enthalpy data based on formation temperature (5-Feb-97). Shut-in pressure data based on WHP on bleed in 2013.
PPL-01 AST	Inj.	1290	-329	1908	1270	470	1223, 1212, 1046, 657, 640, 560, 554, 498, 113	n/a	13.1	Shut-in pressure data based on WHP on bleed in 2013.
PPL-01 BST	Inj.	1321	320	1863	1282	484	676, 605	n/a	11.2	Shut-in pressure data based on WHP on bleed in 2013.
PPL-02	Prod.	1252	13	1849	1229	517	1095, 1043, 754, 700, 626	2760-2065	23.0	Feed zone confirm by spinner survey (18-Sep-2015). Enthalpy data based on TFT measurement 2015 at 8.6-8.9 barg, while PT data in 2015 at 9.2 barg. Shut-in pressure data based on WHP on bleed in 2013
PPL-02 AST	Prod.	1257	371	1869	1189	n/a	1157	2803	23.8	Enthalpy data based on formation temp. (24-Sep-97). Shut-in pressure data based on WHP on bleed in 2013.
PPL-03	Prod.	1175	778	1684	1200	n/a	960, 858	2802	16.3	Enthalpy data based on formation temp. (24-Aug-97). Shut-in pressure data based on WHP on bleed in 2013.
PPL-03 AST	Prod.	1239	1062	1683	1359	n/a	1204	2803	21.0	Enthalpy data based on formation temp. (23-Aug-97). Shut-in pressure data based on WHP on bleed in 2013.
PPL-03BST	Prod.	1250	900	1605	1241	n/a	1050, 1000, 968	2802	21.7	Enthalpy data based on formation temp. (23-Aug-97). Shut-in pressure data based on WHP on bleed in 2013.
PPL-04 ST	Prod.	858	280	1866	1012	n/a	749	2797	12.8	Enthalpy data based on predicted formation temp. (assumed that pure steam flows from well). Shut-in pressure data based on WHP on bleed in 2013.
PPL-04 AST	Idle	n/a	n/a	1860	n/a	n/a	n/a	n/a	?	Suspended well.
PPL-05 ST	Prod.	1317	451	1716	1333	506	1096, 898, 802	2801	22.1	Feed zone confirm - spinner survey 18-Sep -2015. Enthalpy data based on formation temp. (25-Jan-98). Shut-in pressure data based on WHP on bleed in 2013.
PPL-06ST	Prod.	1335	-358	1932	1237	410	1265, 752, 261	2801	20.6	Enthalpy data based on predicted formation temp. (assuming pure steam flow from the well). Shut-in pressure data based on WHP on bleed in 2013.
PPL-07 ST	Prod.	1212	544	1434	1087	736	775	2803	26.2	Feed zone based on profile temperature while heating up. Enthalpy data based on formation temp. (3-Feb-98). Shut-in pressure data based on WHP on bleed in 2013.
PPL-08	Idle	n/a	n/a	2137	n/a	n/a	n/a	n/a	-0.3	Suspended well. Shut-in pressure data based on WHP on bleed in 2013.

Note : TOL = Top of liner; BOL = Bottom of liner

7. CONTOUR MAPS SHOWING TEMPERATURE AND PRESSURE DISTRIBUTION

The slim and deep hole initial temperature and pressure estimates were plotted at several depths in the larger Patuha area. In addition to the real well data, a 40 km diameter circle of hypothetical thermal gradient wells was added to the temperature maps. These are assigned true elevation and always the same linear gradient of 40°C/km. Such an approach will bend temperature contours down from the mid field local high, and therefore provide a conservative estimate of the area extent. The locations of the hypothetical wells are shown in Figure 10.

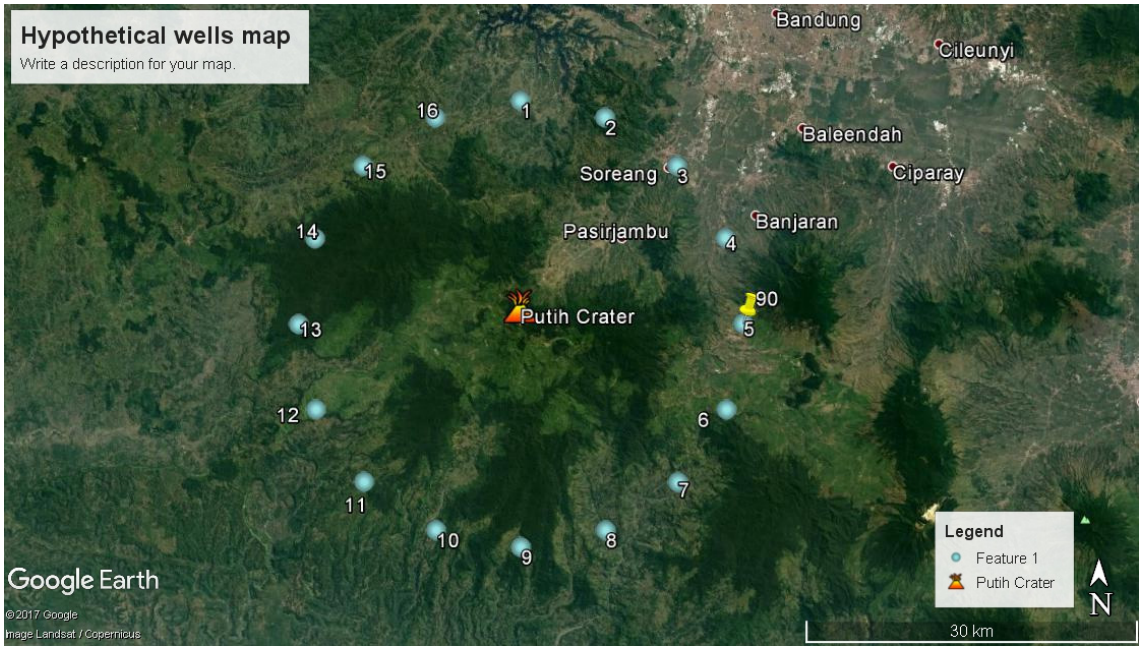

FIGURE 10: Location of hypothetical thermal gradient wells

Figures 11-16 show maps of the temperature distribution in Patuha, in intervals of 250 m from 1750 to 500 m a.s.l. These maps are generated in ArcGIS 10.3 for desktop software developed by ESRI. The method of interpolation is that of natural neighbour. Note the map extent shown is much smaller than in Figure 10. The hypothetical well temperatures nevertheless still support the contour algorithm.

At 1750 m a.s.l. the temperature distribution shows an indication of high temperature around Putih Crater (Figure 11). At 1500 m a.s.l., the highest temperature area is also around Putih Crater, and the >100°C temperature region has now extended to Ciwidey Crater, Cibuni Crater, 07ST and well 03 (Figure 12). At 1250 m a.s.l., a temperature of 200°C is distributed at Putih Crater, Cibuni Crater, 01, 02, 02AST, 03, 03AST, 03BST, 04ST, 05ST, 06ST (Figure 13). At 1000 m a.s.l., a temperature of 220°C is distributed at Putih Crater, near Cibuni Crater, and all wells except 01AST, 01BST, 06ST, and 08 (Figure 14). As well 08 does not reach 1000 m a.s.l., contouring near the well shows less than 220°C.

Wells 01AST, 01BST, and 06ST have reversed temperature beneath the convection zone which infers that these wells are targeting the boundary of reservoir. At 750 m a.s.l., the 220°C temperature contour includes Putih Crater, Cibuni Crater, and all wells except 01, 01AST, 01BST, and 05ST, which are located in the eastern part of the field (Figure 15). At this elevation, well 05ST reaches more than 220°C, but since there is no data at this elevation in 03BST the contour only interpolates until Pad 3. At 500 m a.s.l., the 220°C temperature contour includes Putih Crater, vicinity of Cibuni Crater, and wells in 02, 02AST, 03AST, 04ST, 06ST, and 07ST (Figure 16). The high temperature at 500 m a.s.l. in well 06ST is questionable, since the well has a reverse temperature profile above 500 m a.s.l. This may be affected by data in TCH-07.

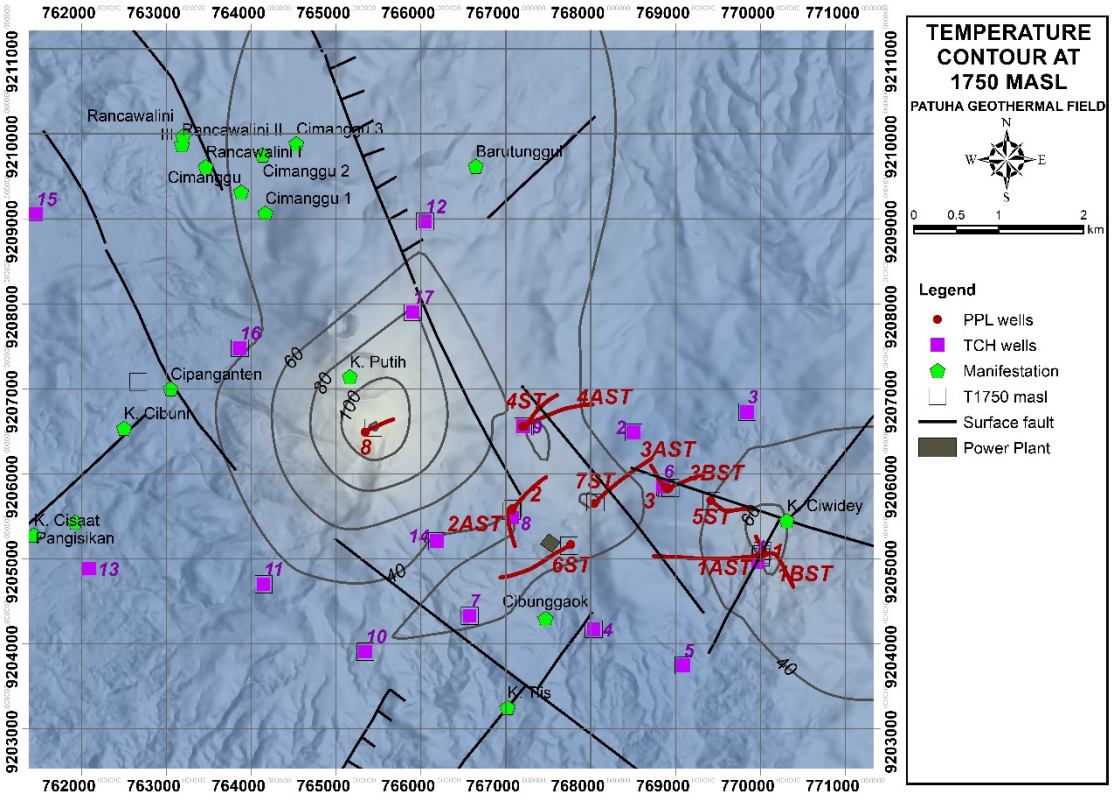

FIGURE 11: Patuha geothermal field, temperature contours at 1750 m a.s.l.

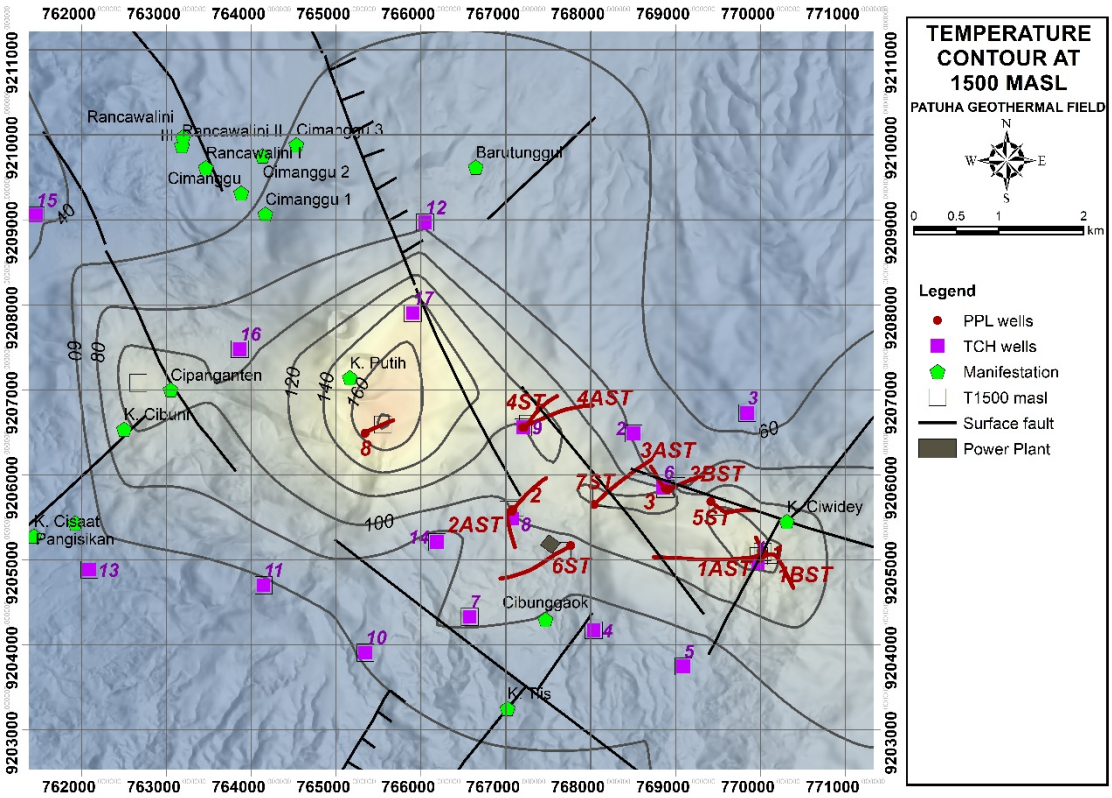

FIGURE 12: Patuha geothermal field, temperature contours at 1500 m a.s.l.

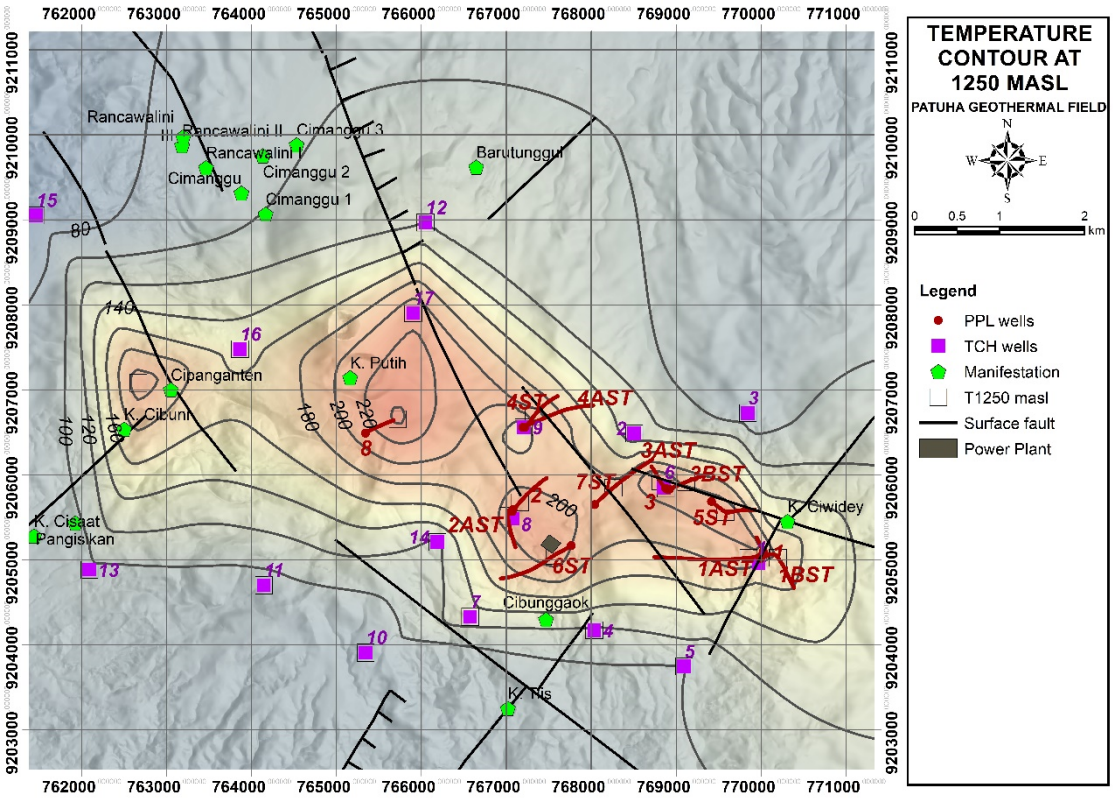

FIGURE 13: Patuha geothermal field, temperature contours at 1250 m a.s.l.

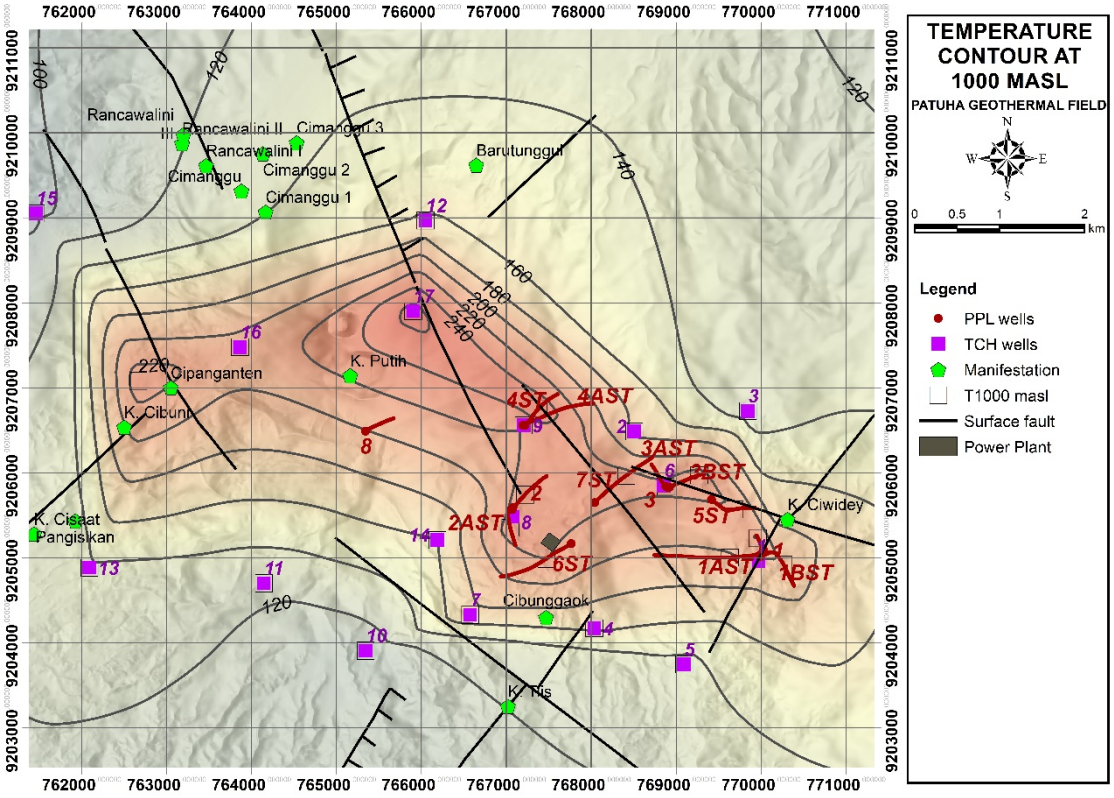

FIGURE 14: Patuha geothermal field, temperature contours at 1000 m a.s.l.

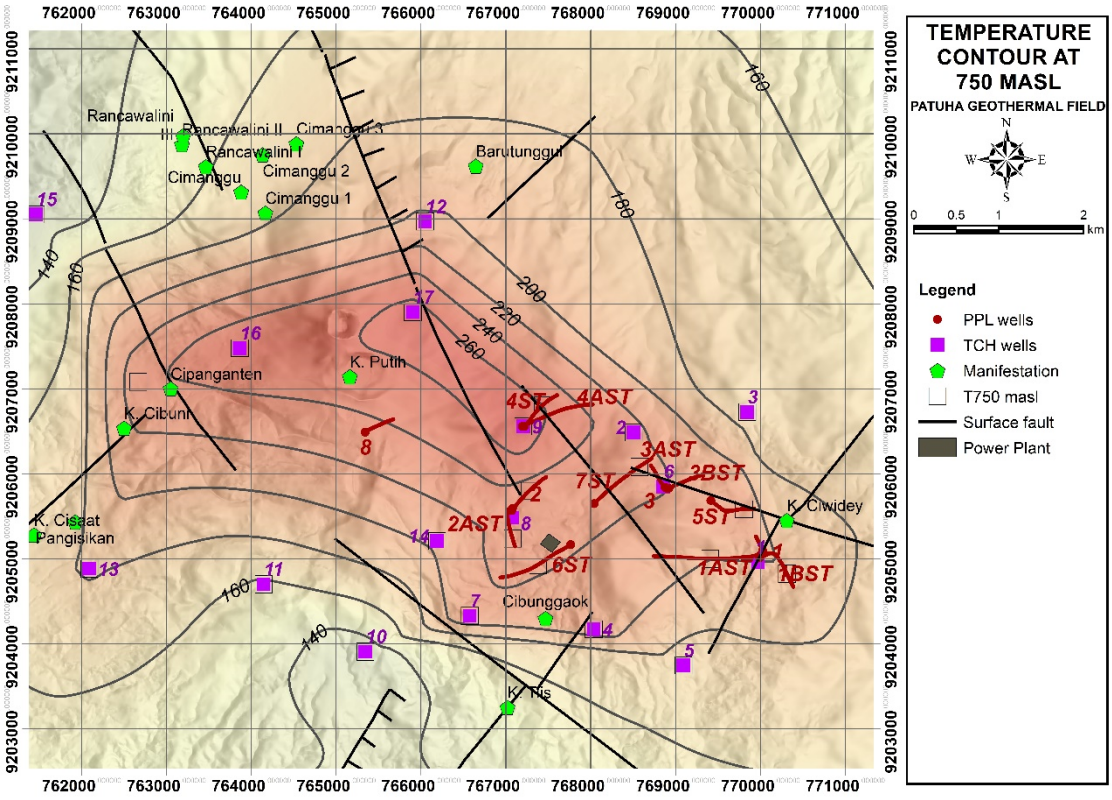

FIGURE 15: Patuha geothermal field, temperature contours at 750 m a.s.l.

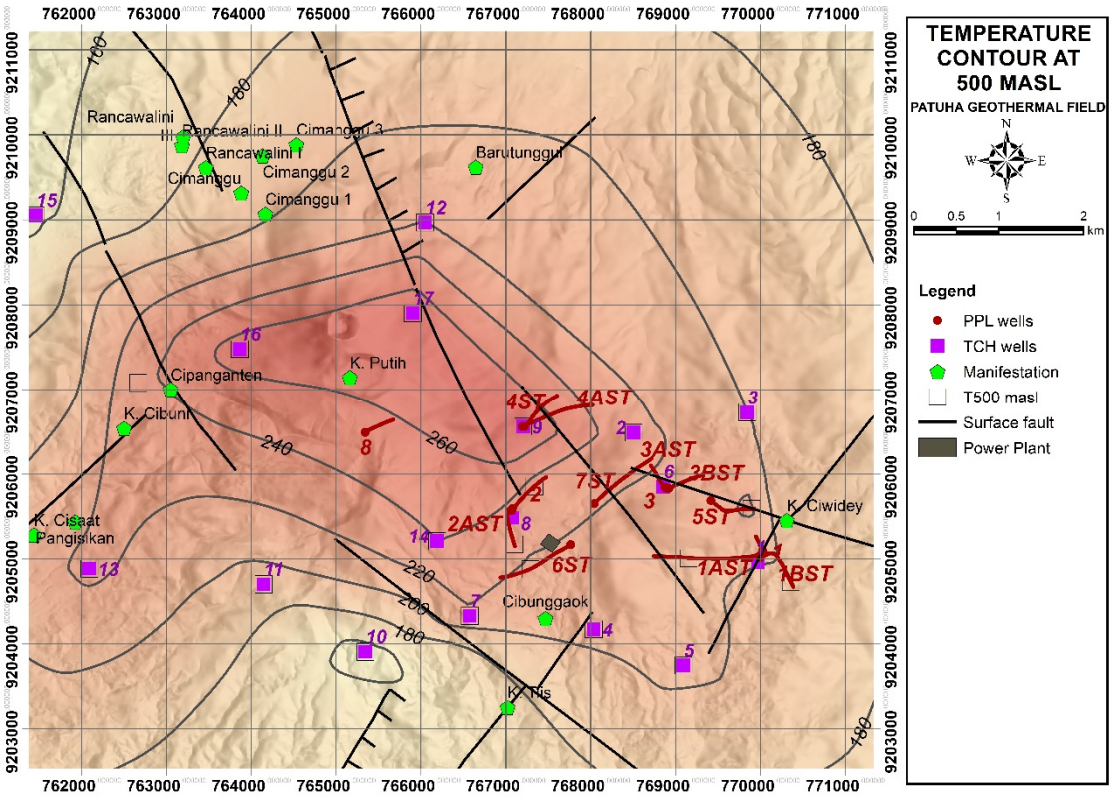

FIGURE 16: Patuha geothermal field, temperature contours at 500 m a.s.l.

In addition to temperature data, the pressure contour map in Figure 17 shows a significant pressure difference between Putih Crater and Ciwidey Crater. It explains the flow pattern of reservoir fluid from the centre of Putih Crater to Cibuni Crater and Ciwidey Crater. The lateral pressure gradient seen within the steam cap from west to east can have several explanations. One reason may be separate upflows, as considered in PT Geo Dipa Energi in house model (PWC et al., 2013).

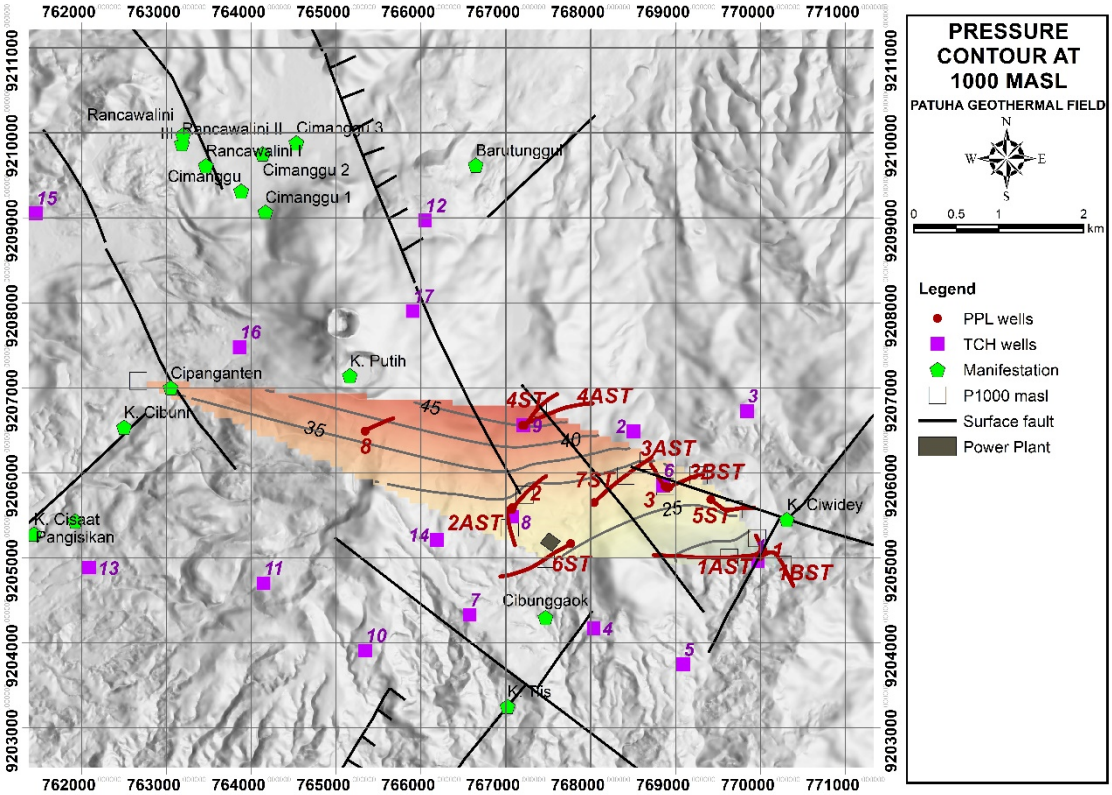

FIGURE 17: Patuha geothermal field, pressure contours at 1000 m a.s.l. and flow pattern in the geothermal reservoir

The temperature reversal in 01AST, 01BST, and 06ST suggests a single upflow zone at Putih Crater and lateral flow to the east-southeast. The lateral steam cap pressure gradient from 50 barg at Putih Crater to less than 20 barg in the easternmost wells then remains to be explained. One explanation is that some of the major faults dissecting the flow channel away from the Putih Crater are behaving as barriers, and thus the steam cap may be explained as being compartmentalised. The reservoir is then losing mass at the east boundary, via fumaroles on surface.

8. LITHOLOGICAL CROSS-SECTION AND FEED ZONES

The following summarizes information on the lithology of the Patuha wells:

- *Wells 01, 01AST, and 01BST*: The lithology consists of the Q_l unit (pyroclastic and thick andesite) and the Q_{Tv} lithology unit (andesite complex) with the appearance of microdiorite intrusions at several depths.
- *Wells 02 and 02AST*: The lithology consists of the Q_v unit (intercalated of pyroclastic, andesitic-dacitic lava, and lithic tuff), the Q_l unit (thick andesite, andesite breccia, and tuff breccia), and the Q_{Tv} unit (andesite complex and breccia/tuff breccia) with samples of microdiorite intrusions at several depths.

- *Wells 03 and 03BST:* Here, the lithology consists of the Q_v unit (intercalated of pyroclastic, andesitic-dacitic lava, and lithic tuff), the Q_l unit (thick andesite, andesite breccia, and tuff breccia), and the Q_{Tv} unit (andesite complex and breccia/tuff breccia) with samples of microdiorite intrusions at several depths.
- *In well 03AST*: the lithology only consists of the Q_v unit (intercalated of pyroclastic, hornblende andesitic, and lithic tuff) and the Q_l unit (thick andesite and tuff breccia).
- *Wells 04ST and 04AST:* Here the lithology consists of the Q_v unit (intercalated of pyroclastic and thin andesite), the Q_l unit (thick andesite, pyroclastic, and tuff breccia), and the Q_{Tv} unit (andesite complex and breccia/tuff breccia) with samples of microdiorite intrusions at several depths and hematized rock.
- *In well 05ST*: the lithology consists of the Q_v unit (intercalated of pyroclastic and andesitic/dacitic lava), the Q_l unit (thick andesite/andesite breccia,), and the Q_{Tv} unit (andesite complex and breccia) with samples of microdiorite intrusions at several depths.
- *In well 06ST*: the lithology consists of the Q_v unit (intercalated of pyroclastic, andesitic-dacitic lava, and hornblende andesite), the Q_l unit (thick andesite, lithic tuff/tuff breccia), and the Q_{Tv} unit (andesite complex) with samples of microdiorite intrusions at several depths.
- *Well 07ST*: the lithology consists of the Q_v unit (andesitic/dacitic rock), the Q_l unit (thick andesite), and the Q_{Tv} unit (thick microdiorite and andesite). Presumably, this well enters the body of the microdiorite intrusion.
- *Well 08*: consists of the Q_v unit (intercalated of pyroclastic), the Q_l unit (thick andesite and tuff breccia), and the Q_{Tv} unit (andesite lava and tuff breccia with samples of microdiorite intrusions in several depths).

Figure 18 shows a geological cross-section from west to east. It is based on the geophysical cross-section, but focuses only on the eastern part, since no lithological data was available for this study from wells in the western part. In the previous discussion about the analysis of downhole data, it can be seen that the reservoir is distributed within the Q_l and Q_{Tv} lithology units. Almost all the feed zones are in the Q_{Tv} lithology unit, which consists of andesite complex (andesite lava associated with microdiorite), andesite breccia, and breccia / tuff breccia. The main difference of Q_{Tv} compared to the other lithology units is microdiorite as an intrusion rock. Enhanced permeability within this lithology unit is presumably affected by contact between the intrusions and the host rock. Therefore, the lithology unit controls the distribution of reservoir and permeability (Figure 18). Aside from the distance between Putih Crater and

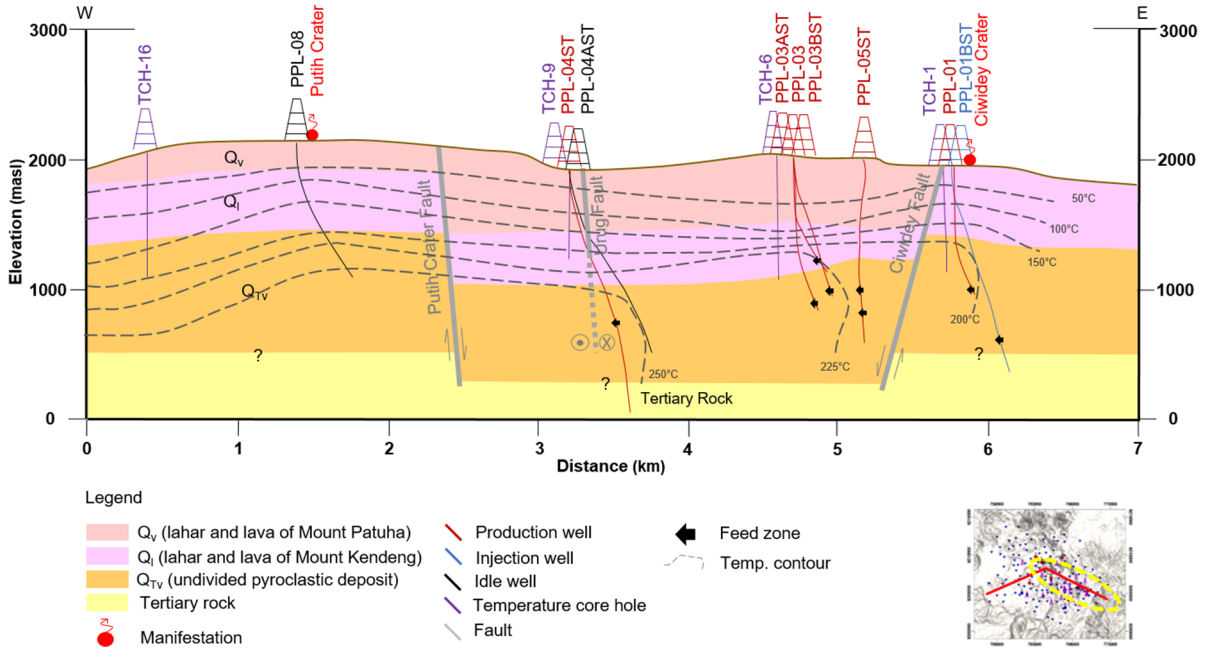

FIGURE 18: Patuha geothermal field, a W-E temperature and geological cross-section

Ciwidey Crater, the Ciwidey Crater Fault and Putih Crater Fault presumably have control of the pressure drop from Putih Crater to Ciwidey Crater. If the main control on the permeability is in the lithology unit, then Putih Crater Fault creates a discontinuity of flow inside Q_{Tv} to the eastern part. Ciwidey Crater Fault may also create "leakage" for steam to the surface. Presumably, this "leakage" also creates a pressure drop in the reservoir sector hosting wells 01, 01AST, and 01BST.

9. THE CONCEPTUAL RESERVOIR MODEL

A previous conceptual model by Layman and Soemarinda (2003) explains that the major components in Patuha geothermal field are a steam reservoir, liquid zone, magmatic plume zone, and a shallow thermal aquifer (Figure 19). An indication of a magmatic plume beneath the Putih Crater is the acidic, high salinity, with sulphur precipitation at the surface near the fumaroles. The flow pattern of the steam reservoir is controlled by a west-northwest trending structure.

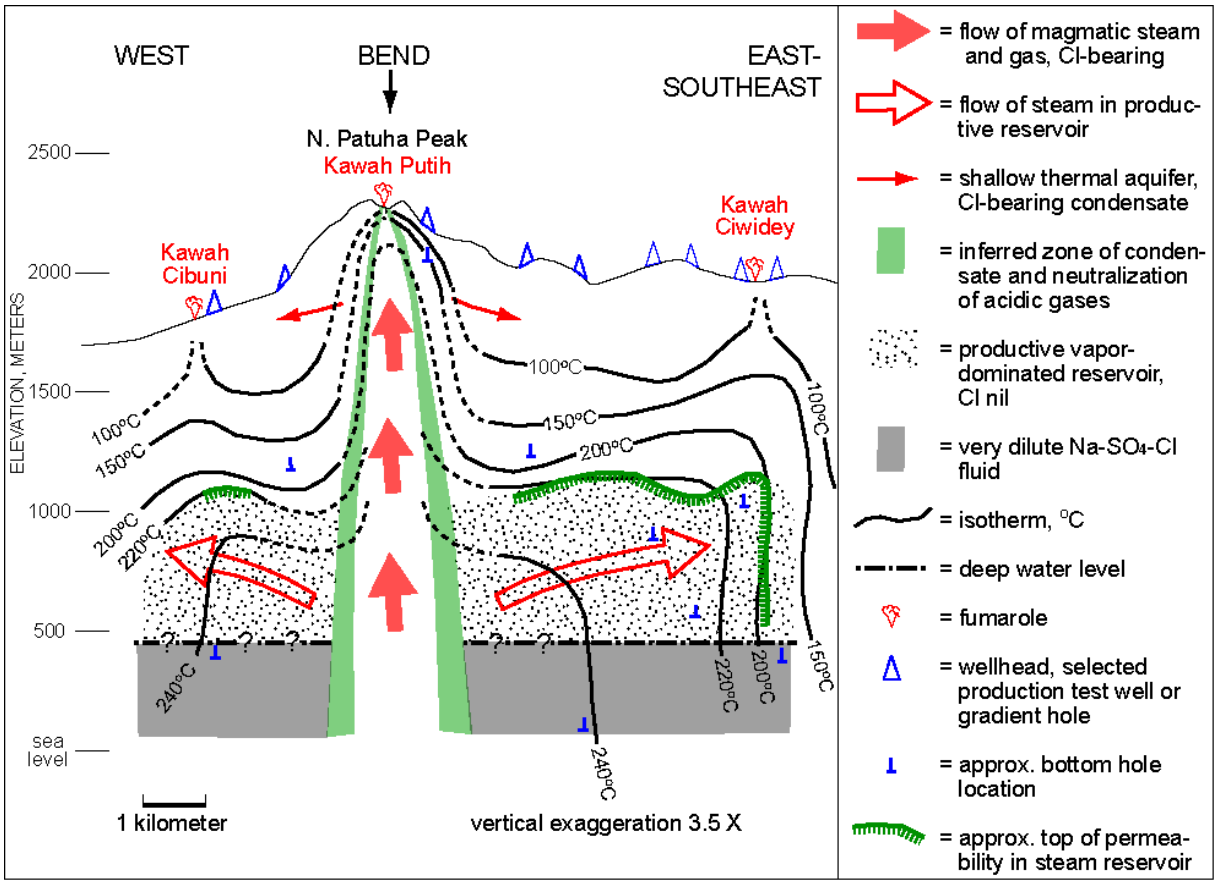

FIGURE 19: Conceptual model of the Patuha geothermal field by Layman and Soemarinda (2003)

A lot of new field data and data analysis have been collected since Layman and Soemarinda presented their conceptual model in 2003. Most important here is an updated MT resistivity model (Figure 5), more downhole pressure and temperature data, and finally the reservoir response to production after commissioning the 55 MW Patuha power plant in 2014.

Figure 20 is therefore an update to the conceptual model in Figure 19. The figure shows a cross-section drawn identically to that in Figure 5. A single-upflow zone is shown under Putih Crater, consisting of magmatic fluid of low resistivity (shown in red). A relative flat boundary between the steam cap and the underlying water reservoir is presented. This is speculative, as only a handful of wells reach this part of the reservoir.

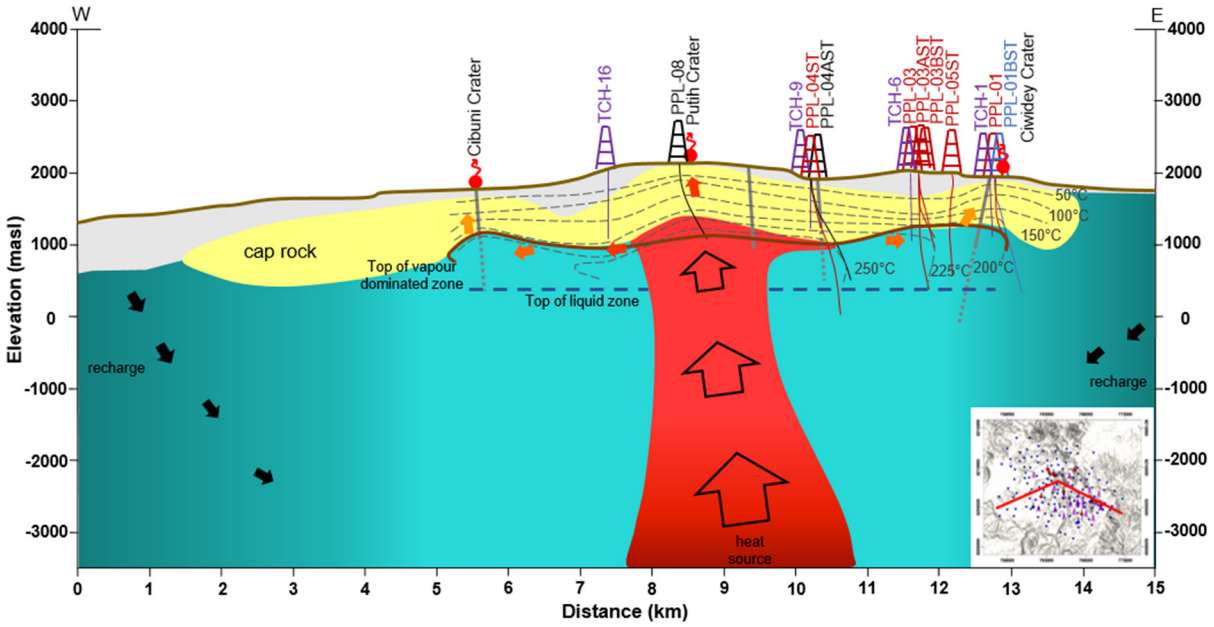

FIGURE 20: Updated conceptual model for the Patuha geothermal field

Although the pressure data from the wells is incomplete, an indication of the flow pattern from Putih Crater as upflow to the east is clearly shown. The thickness of the cap rock increases to the northern, north-western, and western parts of the field. Cap rock below Putih Crater, Pad 3, Pad 5 and Cibuni Crater is relatively thinner compared to other areas.

Generally, in high terrain geothermal systems, fumaroles represent the upflow zone (Nicholson, 1993). Nevertheless, this may not be the case for Ciwidey and Cibuni Crater. The fumaroles in Ciwidey and Cibuni Crater are located in an outflow zone. This is confirmed by PT logs, and in those areas the temperature and pressure are lower compared to Putih Crater. Particularly in Ciwidey Crater, the pressure is low, less than 20 barg, and the temperature is also lower compared to other areas. The Ciwidey and Cibuni Crater Faults seem to have high permeability, however, these faults also block the high-temperature distribution from extending further. Hot and warm springs in north and south areas, around elevation 1700 m a.s.l., are connected with shallow ground water that is detected in the wells, mostly around 1800-1700 m a.s.l.

The reservoir is distributed within the Q_l and Q_{Tv} lithology units and almost all the feed zones are in the Q_{Tv} lithology unit. It is presumed that the Q_{Tv} lithology unit is the main control of permeability. The reservoir in this field can be divided into two zones, i.e. upper vapour-dominated zone and deeper liquid-dominated zone. The liquid zone is probably distributed within Tertiary rocks. The temperature of the vapour-dominated zone ranges from 220 to 260°C and its thickness varies between 220 and 830 m. The temperature reserve in 01AST, 01BST, and 06ST also indicates the boundary of the reservoir in the eastern and southern part.

As the deep reservoir pressure potential is very low when compared with surface, the edges of the system are supposed to be tight. Therefore, peripheral cold water cannot influence the vapour zone. These indications show that the system is sealed (Layman and Soemarinda, 2003) and limited.

10. KEY PARAMETERS FOR VOLUMETRIC MODELLING

Volumetric assessment can be used to estimate roughly the resource generating capacity of Patuha geothermal field. The analysis of the temperature distribution presented here actually provides an

estimate for many of the reservoir parameters that govern the volumetric models. Note that as the volumetric model is based on actual temperature data, it can be classified as a proven reserve estimate, contrary to the possible and probable models where deep temperatures are estimated by geochemistry and extrapolating shallow well temperatures. In the current work an in-house ÍSOR volumetric modelling software is used (written by Gunnar Thorgilsson).

The main composition of the rock in the reservoir is andesitic. The reservoir area is estimated from Table 4 taking areas with temperatures above 220°C. This yields a minimum area of 6.6 km^2 and maximum of 20.2 km^2. Predicted maximum reservoir temperature is 260°C and minimum reservoir temperature is 220°C. The input parameter of temperature is only based on well data, from wells which mostly enter the vapour-dominated zone and limited data for the liquid zone. The minimum reservoir thickness is the thickness of the vapour-dominated zone. The most likely and maximum reservoir thickness includes both the vapour-dominated and the liquid zone. The input parameters for the volumetric modelling are detailed in Figure 21, and the outcome of the model analysis is shown in Figures 22 and 23. This study infers a reserve capacity exceeding the currently installed 55 MW power plant. Due to the many simplifications and assumptions made, this model should, however, only be used as a reference. A more complex 3D reservoir model is a better approach.

TABLE 4: Reservoir area at different elevation

Elevation (m a.s.l.)	Area with temperature (km^2)		
	220°C	240°C	260°C
1000	6.6	2.4	0.5
750	13.8	6.4	1.8
500	20.2	9.4	3.2

Rock Type:	Andesite	Number of Monte Carlo runs	10000
Display output distribution in:	MegaWatts	Number of bins in Histograms	100
Show pop-up plots?	Yes	Time of energy usages [years]	30

	Min	Best Value	Max	Distribution type
Area [km^2]	6.6	13.8	20.2	Triangular distribution
Thickness [m]	900	1500	2000	Triangular distribution
Temperature [C°]	220	240	260	Triangular distribution
Porosity [%]	5	10	15	Triangular distribution
Specific heat of rock [J/(kg C°)]	N/A	1000	N/A	Triangular distribution
Density of rock [kg/m^3]	2500	N/A	2800	Constant distribution
Specific heat of water [J/(kg C°)]	N/A	4510	N/A	Fixed value
Density of water [kg/m^3]	N/A	813	N/A	Fixed value
Recovery factor [%]	N/A	25	N/A	Fixed value
Cut-off temperature [C°]	N/A	180	N/A	Fixed value
Efficiency [%]	N/A	10	N/A	Fixed value
Load factor [%]	N/A	95	N/A	Fixed value

FIGURE 21: Input parameters in volumetric calculation for Patuha

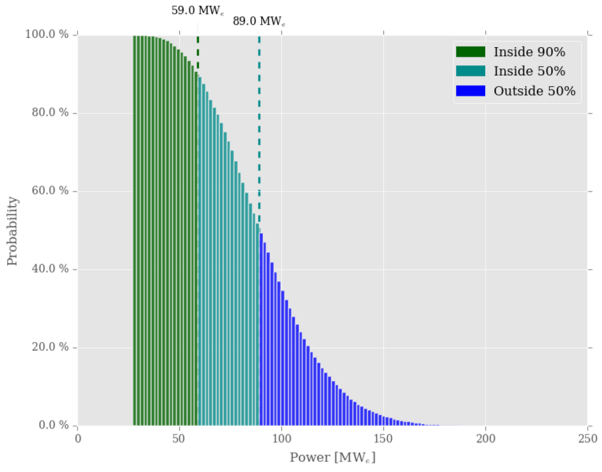

FIGURE 22: Cumulative output histogram for the volumetric model for Patuha

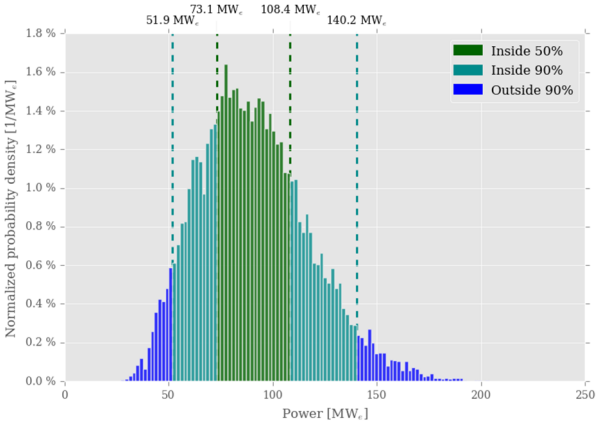

FIGURE 23: Normalized probability density for the volumetric model for Patuha

11. DISCUSSION

A conceptual model and numerical simulation for a vapour-dominated system has been described by Ingebritsen and Sorey (1988). Such systems are generally under-pressured compared to local hydrostatic pressure. Condensate zone is overlying a vapour-dominated zone and a high-temperature liquid zone is underlying the vapour-dominated zone. This model can describe the Patuha reservoir, which also has a liquid zone underneath the vapour-dominated zone. Additionally, the liquid zone can be used for production to enhance the vapour zone recharge. Although there is no evidence that this mechanism supports the vapour zone in Patuha, spinner data in well 02 shows the liquid also can be used for production. There are two processes that can produce an extensive vapour-dominated zone. The first process is decreasing the mass inflow and the second process is that of an in-boundary condition with a constant rate conductive heating (Ingebritsen and Sorey, 1988).

Modelling of vapour-dominated systems have also been carried out by Raharjo (2016). Raharjo uses five known vapour-dominated fields in Java for modelling assumptions. The early stage of simulation shows that a liquid-dominated reservoir is developed. The second stage is a conversion from liquid to steam assumed to start at 6 kyr (thousand years). While the vapour-dominated zone starts to develope at a pressure of 40-50 barg, the pressure drops and the temperature increases in the liquid zone below it. At vapour saturation of 64%, the liquid zone becomes immobile in compliance with the used relative permeability relationship (Figure 24). In this scenario, the vapour-dominated zone is expanding down to more than 1.5 km depth at 9.7 kyr. Consequently, the reservoir pressure in the vapour-dominated zone and the liquid zone becomes lower compared to the initial hydrostatic pressure (Figure 25).

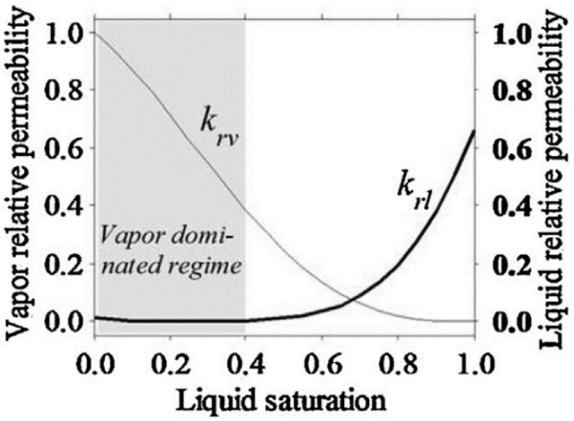

FIGURE 24: Relative permeability curves assumed in the Java vapour-dominated model study (Raharjo et al., 2016)

In general, therefore (Ingebritsen and Sorey, 1988 and Raharjo et al., 2016), vapour-dominated systems evolve from liquid-dominated systems. The process, which controls the production of the extensive

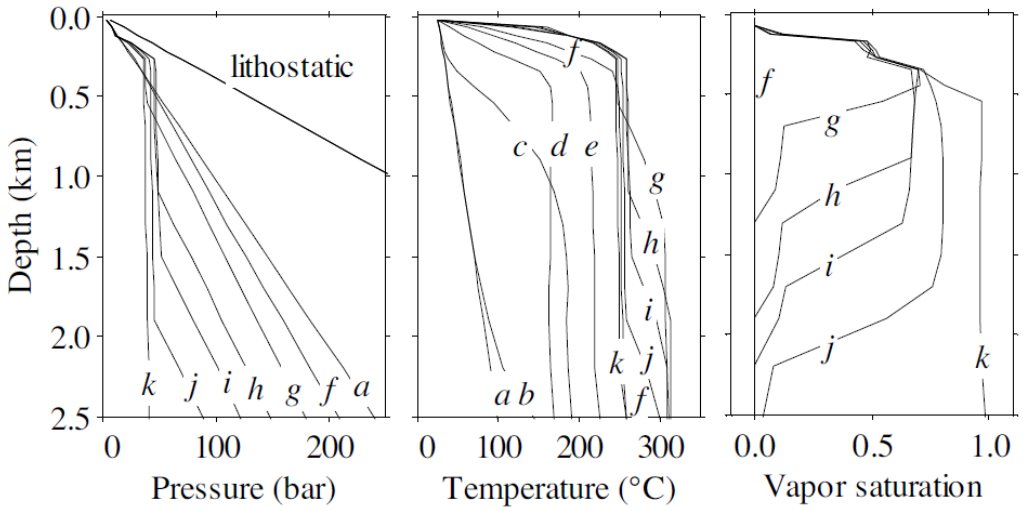

FIGURE 25: Evolution of pressure, temperature, and vapour saturation for basal heat strength 8 MW/km^2 in a vapour-dominated system (Raharjo et al., 2016)

vapour-dominated zone in Patuha, is still unknown and future work should aim at trying to understand this mechanism in the natural state model. The Patuha liquid zone underlying the vapour-dominated zone (Figure 21) is also demonstrated in Figure 25. Although the model shows that the liquid zone is immobile, well data confirms some contribution of the liquid zone to the well flow. The liquid zone seems to support the vapour-dominated zone if the pressure drops in the liquid zone. The same phenomenon also occurs in Svartsengi geothermal field, the pressure drop in the reservoir generates the expansion of a two-phase zone (Björnsson and Steingrímsson, 1992).

In the early years of Patuha production, a decline of some steam wells was observed. A future challenge is therefore to maintain the steam supply for additional 30 years. The deep reservoir liquid zone looks attractive as an option in the future resource management.

12. CONCLUSIONS

The Patuha geothermal field is surrounded by a central volcano that trends along west to northwest. Regional compression from north to south produces NW-SE dextral strike-slip faults, NE-SW sinistral strike-slip faults, and normal faults. High permeability faults control the appearance of the fumaroles in Ciwidey and Cibuni craters. The regional geology map becomes the main reference to help produce a simplified lithology structure in the well field.

The review of structure, lithology, and PT logs in the wells has led to following conclusions:

1. Some faults control the permeability of the reservoir, particularly Cibuni, Putih, and Ciwidey Crater faults. Faults at the edge of the reservoir behave as tight boundaries. Faults also appear to compartmentalise the main reservoir and explain the sizeable lateral pressure gradients from west to east.
2. The reservoir and feed zones are mostly associated with the Q_{Tv} lithology unit, the main difference of Q_{Tv} compared to other lithology units is microdiorite as intrusion rock. Enhanced permeability in this lithology unit is presumably affected by the contact between the intrusions with the host rock. Therefore, the lithology unit probably is the main control on the distribution of the reservoir and permeability.
3. The 220-260°C productive reservoir in this field can be divided into two zones, i.e. upper vapour-dominated zone and deeper liquid-dominated zone. Most feed zones in the production wells are located in the vapour-dominated zone, but several wells also enter the liquid zone.
4. The reverse temperature profiles in eastern and southern part indicate outer boundary of the reservoir.
5. A cross correlation of temperature, pressure and resistivity models infers a single upflow zone beneath the Putih Crater.
6. A volumetric resource assessment is consistent with the current 55 MW power plant capacity.
7. One option in maintaining the current power plant output is to produce more from the deep liquid zone, thereby dropping its pressure and flash the resulting steam into the vapour zone.

ACKNOWLEDGEMENTS

I would like to express my gratitude to my supervisors, Mr. Grímur Björnsson for reviewing this project, encouragement, and his expert advice; and Ms. Valdís Gudmundsdóttir and Mr. Gunnar Thorgilsson for their review on the draft and suggestions. I am particularly grateful for this training experience, support, and assistance given by the UNU-GTP staff, Dir. Lúdvík S. Georgsson, Mr. Ingimar Gudni Haraldsson, Ms. Málfrídur Ómarsdóttir, Ms. Thórhildur Ísberg and Mr. Markús A.G. Wilde. Special thanks to my company PT Geo Dipa Energi (Persero) and all my colleagues in the Engineering Division for giving permission and full support.

REFERENCES

Björnsson, G., and Steingrímsson, B., 1992: Fifteen years of temperature and pressure monitoring in the Svartsengi high-temperature geothermal field in SW-Iceland. *Geothermal Resources Council Transactions, 16*, 627-633.

Bogie, I., Kusumah, Y.I., and Wisnandary, M.C., 2008: Overview of the Wayang Windu geothermal field, West Java, Indonesia. *Geothermics, 37*, 19 pp.

Elfina, 2017: *Estimated initial temperatures and pressures in all deep Patuha wells*. PT Geo Dipa Energi (Persero), Indonesia, internal report, 17 pp.

Elnusa, 2013: *Reprocessing MT-TDEM and gravity in the Dieng and Patuha geothermal fields*. PT GeoDipa Energi (Persero), Indonesia, internal report (in Indonesian), 254 pp.

Fauzi, A., Permana, H., Indarto, S., and Gaffar, E.Z, 2015: Regional structure control on geothermal systems in West Java, Indonesia. *Proceedings of the World Geothermal Congress 2015, Melbourne, Australia,* 14 pp.

Geosystem, 1995: *Geophysics in the Patuha area West Java, Republic of Indonesia*. Geosystem, SRL, PT GeoDipa Energi (Persero), internal report, 32 pp.

Geosystem, 1996: *Gravity survey, Patuha West Java, Republic of Indonesia*. Geosystem SRL, PT GeoDipa Energi (Persero), internal report, 37 pp.

Hall, R., 2012: Late Jurassic-Cenozoic reconstruction of the Indonesian region and the Indian Ocean. *Tectonophysics, 570-571,* 41 pp.

Ingebritsen, S.E., and Sorey, M.L., 1988: Vapor-dominated zones within hydrothermal system: evolution and natural state. *J. Geophysical Research, 93*, 13635-13655.

JBIC, 2007: *Feasibility study for Patuha geothermal power development.* PT Geo Dipa Energi (Persero), Indonesia, internal report, 276 pp.

Koesmono, M., Kusmana, and Suwarna, N., 1996: *Geological map of the Sindangbarang and Bandarwaru quadrangles, Java* (2nd ed.). Geological Research and Development Centre, Indonesia.

LAPI ITB, 2014: *Report on structural geological survey in Patuha geothermal field*. PT Geo Dipa Energi (Persero), Indonesia, internal report (in Indonesian), 182 pp.

Layman, E.B., and Soemarinda, S., 2003: The Patuha vapor-dominated resource West Java, Indonesia. *Proceeding of the 28th Workshop on Geothermal Reservoir Engineering, Stanford University, Stanford, CA,* 10 pp.

Nicholson, K., 1993: *Geothermal fluids: chemistry and exploration techniques*. Springer-Verlag, Berlin Heidelberg, 278 pp.

PWC, ELC, Hadiputranto, Hadinoto & Partners, and Mandiri Sekuritas, 2013: *Final report - consultant's services for the development of the Dieng geothermal area units 2 & 3 and Patuha units 2 & 3*. PT Geo Dipa Energi (Persero), Indonesia, internal report, 429 pp.

Raharjo, I.B., Allis, R.G., and Chapman, D.S., 2016: Volcano-hosted vapour-dominated geothermal system in permeability space. *Geothermics, 62*, 22-32.

Reyes, A.G., 2000: *Petrology and mineral alteration in hydrothermal system: from diagenesis to volcanic catastrophes*. UNU-GTP, Iceland, report 1998-18, 77 pp.

Satyana, A.H., 2007: Central Java, Indonesia – A "terra incognita" in petroleum exploration: new consideration on the tectonic evolution and petroleum implications. *Proceedings of the Indonesian Petroleum Association 31st Annual Convention and Exhibition, Indonesia*, 22 pp.

Sriwana, T., Van Bergen, M.J., Varekamp, J.C., Sumarti, S., Takano, B., Van Os, B.J.H., and Leng, M.J., 2000: Geochemistry of the acid Kawah Putih lake, Patuha volcano, West Java, Indonesia. *J. Volcanology & Geothermal Research, 97,* 77-104.